High-precision quark masses and QCD coupling from $n_f = 4$ lattice QCD

Bipasha Chakraborty,[1] C. T. H. Davies,[1] B. Galloway,[1] P. Knecht,[1] J. Koponen,[1]
G. C. Donald,[2] R. J. Dowdall,[3] G. P. Lepage,[4,*] and C. McNeile[5]

(HPQCD Collaboration)

[1]*SUPA, School of Physics and Astronomy, University of Glasgow, Glasgow G12 8QQ, United Kingdom*
[2]*Institut für Theoretische Physik, Universität Regensburg, 93040 Regensburg, Germany*
[3]*DAMTP, University of Cambridge, Wilberforce Road, Cambridge, CB3 0WA United Kingdom*
[4]*Laboratory for Elementary-Particle Physics, Cornell University, Ithaca, New York 14853, USA*
[5]*School of Computing and Mathematics and Centre for Mathematical Science, Plymouth University,
Plymouth PL4 8AA, United Kingdom*

We present a new lattice QCD analysis of heavy-quark pseudoscalar-pseudoscalar correlators, using gluon configurations from the MILC Collaboration that include vacuum polarization from u, d, s, and c quarks ($n_f = 4$). We extract new values for the QCD coupling and for the c quark's $\overline{\text{MS}}$ mass: $\alpha_{\overline{\text{MS}}}(M_Z, n_f = 5) = 0.11822(74)$ and $m_c(3 \text{ GeV}, n_f = 4) = 0.9851(63)$ GeV. These agree well with our earlier simulations using $n_f = 3$ sea quarks, vindicating the perturbative treatment of c quarks in that analysis. We also obtain a new nonperturbative result for the ratio of c and s quark masses: $m_c/m_s = 11.652(65)$. This ratio implies $m_s(2 \text{ GeV}, n_f = 3) = 93.6(8)$ MeV when it is combined with our new c mass. Combining m_c/m_s with our earlier m_b/m_c gives $m_b/m_s = 52.55(55)$, which is several standard deviations (but only 4%) away from the Georgi-Jarlskop prediction from certain grand unified theories. Finally we obtain an $n_f = 4$ estimate for $m_b/m_c = 4.528(54)$ which agrees well with our earlier $n_f = 3$ result. The new ratio implies $m_b(m_b, n_f = 5) = 4.162(48)$ GeV.

PACS numbers: 11.15.Ha, 12.38.Aw, 12.38.Gc

I. INTRODUCTION

The precision of lattice QCD simulations has increased dramatically over the past decade, with many calculations now delivering results with 1%–2% errors or less. Such precision requires increasingly accurate values for the fundamental QCD parameters: the quark masses and the QCD coupling. Accurate QCD parameters are important for non-QCD phenomenology as well. For example, theoretical uncertainties in several of the most important Higgs branching fractions are currently dominated by uncertainties in the heavy-quark masses (especially m_b and m_c) and the QCD coupling [1].

In this paper we present new lattice results for m_c, m_c/m_s, m_s, m_b/m_c, m_b, and α_s. In a previous paper [2] we obtained 0.6% accurate results for the masses and coupling by comparing continuum perturbation theory with non-perturbative lattice-QCD evaluations of current-current correlators for heavy-quark currents. Current-current correlators are particularly well suited to a perturbative analysis because nonperturbative effects are suppressed by four powers of $\Lambda_{\text{QCD}}/2m_h$ where m_h is the heavy-quark mass. Our earlier simulations treated u, d, and s sea quarks

nonperturbatively ($n_f = 3$), while assuming that contributions from c and heavier quarks can be computed using perturbation theory. Here we test the assumption that heavy-quark contributions are perturbative by repeating our analysis with lattice simulations that treat the c quark nonperturbatively ($n_f = 4$ in the simulation).

In Sec. II we present our new $n_f = 4$ lattice-QCD analysis of current-current correlators, leading to new results for the heavy-quark masses and the QCD coupling. We introduce an improved procedure that gives smaller errors and simplifies the analysis. We also demonstrate how our Monte Carlo data correctly reproduce the running of the $\overline{\text{MS}}$ masses and coupling. In Sec. III, we use the same simulations to calculate a new nonperturbative result for the ratio of the c to s quark masses, m_c/m_s. In Sec. IV, we use these simulations to calculate the mass ratio m_h/m_c for heavy quarks with masses m_h between m_c and m_b. We express the ratio as a function of the heavy quark's pseudoscalar mass m_{η_h}. We extrapolate our result to $m_{\eta_h} = m_{\eta_b}$ to obtain a new nonperturbative estimate for m_b/m_c. In Sec. V, we summarize our conclusions, derive new values for the s and b masses, and present our thoughts about further work in this area. We also include, in Appendix A, a detailed discussion about how the coupling constant, quark masses, and the lattice spacing depend

*g.p.lepage@cornell.edu

upon sea-quark masses in our approach. Our current analysis includes u/d sea-quark masses down to physical values, so we are able to analyze this in far more detail than before. Finally, Appendix B briefly summarizes $n_f = 4$ results obtained using our previous methods [2].

II. LATTICE RESULTS

Our new analysis follows our earlier work [2], but with a simpler and more accurate method for connecting current correlators to $\overline{\text{MS}}$ masses. In particular, this method allows us to determine the $\overline{\text{MS}}$ c mass at multiple scales, from correlators with different heavy-quark masses, providing a new test of our use of continuum perturbation theory. While the lattice spacings are not as small as before, our new analysis treats c quarks in the quark sea nonperturbatively. We also use the substantially more accurate HISQ discretization for the sea-quark action [3], in place of the ASQTAD discretization in our earlier analysis, and a more accurate method for setting the lattice spacing. The gluon action is also improved over our earlier analysis, as it now includes $\mathcal{O}(n_f\alpha_s a^2)$ corrections [4]. Our new results also have more statistics and include ensembles with u/d masses very close to the physical value.

A. Heavy-quark correlator moments

As before, we compute (temporal) moments,

$$G_n \equiv \sum_t (t/a)^n G(t), \tag{1}$$

of correlators formed from the pseudoscalar density operator of a heavy quark, $j_5 \equiv \bar{\psi}_h \gamma_5 \psi_h$:

$$G(t) = a^6 \sum_{\mathbf{x}} (am_{0h})^2 \langle 0|j_5(\mathbf{x}, t)j_5(0, 0)|0\rangle. \tag{2}$$

Here m_{0h} is the heavy quark's bare mass (from the lattice QCD lagrangian), a is the lattice spacing, time t is Euclidean and periodic with period T, and the sum over spatial positions $\mathbf{x}$ sets the total three-momentum to zero. We again reduce finite-lattice spacing, tuning, and perturbative errors by replacing the moments in our analysis with reduced moments,

$$\tilde{R}_n \equiv \begin{cases} G_4/G_4^{(0)} & \text{for } n = 4, \\ \frac{1}{m_{0c}}(G_n/G_n^{(0)})^{1/(n-4)} & \text{for } n \geq 6, \end{cases} \tag{3}$$

where $G_n^{(0)}$ is the moment in lowest-order weak-coupling perturbation theory using the lattice regulator, and m_{0c} is the bare mass of the c quark.

Low-n moments are dominated by short-distance physics because the correlator is evaluated at zero total energy,

which is well below the threshold for on-shell hadronic states: the threshold is at $E_{\text{threshold}} = m_{\eta_h}$ where

$$2.9 \text{ GeV} \leq m_{\eta_h} < 6.6 \text{ GeV} \tag{4}$$

for our range of masses m_{0h}. Furthermore, the moments are independent of the ultraviolet cutoff when $n \geq 4$. Applying the Operator Product Expansion (OPE) to the product of currents in the correlator, we can therefore write our $n = 4$ reduced moment in terms of continuum quantities,

$$\tilde{R}_4 \to r_4(\alpha_{\overline{\text{MS}}}, \mu)\left\{1 + d_4^{\text{cond}}(\alpha_{\overline{\text{MS}}}, \mu)\frac{\langle\alpha_s G^2/\pi\rangle_{\text{eff}}}{(2m_h)^4} \right. \\ \left. + \tilde{d}_4^{\text{cond}}(\alpha_{\overline{\text{MS}}}, \mu)\sum_{q=u,d,s}\frac{\langle m_q\bar{\psi}_q\psi_q\rangle_{\text{eff}}}{(2m_h)^4} + \cdots\right\}, \tag{5}$$

in the continuum limit ($a \to 0$). Here $\alpha_{\overline{\text{MS}}}$ is the $\overline{\text{MS}}$ coupling at scale μ, and m_h is the $\overline{\text{MS}}$ h-quark mass. Heavy-quark condensates are absorbed into the gluon condensate [5]. We will retain terms only through the gluon condensate in what follows since its contribution is already very small and contributions from other condensates will be much smaller. We discuss the precise meaning of $\langle\alpha_s G^2/\pi\rangle_{\text{eff}}$ below. Reduced moments with $n \geq 6$ can be written

$$\tilde{R}_n \to \frac{r_n(\alpha_{\overline{\text{MS}}}, \mu)}{m_c(\mu)}\left\{1 + d_n^{\text{cond}}(\alpha_{\overline{\text{MS}}}, \mu)\frac{\langle\alpha_s G^2/\pi\rangle_{\text{eff}}}{(2m_h)^4} + \cdots\right\}, \tag{6}$$

where $m_c(\mu)$ is the $\overline{\text{MS}}$ mass of the c quark. The continuum expressions for $\tilde{R}_n$ should agree with tuned lattice simulations up to finite-lattice-spacing errors of $\mathcal{O}((am_h)^2\alpha_s)$. The perturbative expansions for the coefficient functions r_n are known through third order: see Table I and [6–10]. The expansions for d_n^{cond} are known through first order [11].

Parameter μ sets the scale for m_c and for $\alpha_{\overline{\text{MS}}}$ in r_n. As in our previous paper, we take

$$\mu = 3m_h(\mu) \tag{7}$$

TABLE I. Perturbation theory coefficients for r_n with $n_f = 4$ sea quarks, where the heaviest sea quark has the same mass m_h as the valence quark (that is, the quark used to make the currents in the current-current correlator). Coefficients are defined by $r_n = 1 + \sum_j r_{nj}\alpha_{\overline{\text{MS}}}^j(\mu)$ where $\mu = m_h(\mu)$. These coefficients are derived in [6–10].

n	r_{n1}	r_{n2}	r_{n3}
4	0.7427	0.0088	−0.0296
6	0.6160	0.4976	−0.0929
8	0.3164	0.3485	0.0233
10	0.1861	0.2681	0.0817

in order to improve the convergence of perturbation theory. In fact, however, our method is almost completely independent of the choice of μ, by design. We can reexpress μ in terms of the $\overline{\text{MS}}$ mass of the c quark,

$$\mu = 3m_c(\mu) \frac{m_{0h}}{m_{0c}}, \tag{8}$$

since the ratios of quark masses are regulator independent, that is,

$$\frac{m_{0h}}{m_{0c}} = \frac{m_h(\mu)}{m_c(\mu)} \tag{9}$$

up to a^2 errors (for any μ).

Our reduced moments differ for $n \geq 6$ from our earlier work; here, we multiply by $1/m_{0c}$ in Eq. (3) instead of $m_{\eta_h}/2m_{0h}$. The ratio of Gs in $\tilde{R}_{n \geq 6}$ introduces a factor of $m_{0h}/m_h(\mu)$. This becomes $1/m_c(\mu)$ when multiplied by $1/m_{0c}$ [by Eq. (9)]. Consequently we can use moments calculated with any heavy-quark mass m_{0h} to estimate the $\overline{\text{MS}}$ c mass [at $\mu = 3m_h(\mu)$]. Consistency among m_cs coming from different m_{0h} values is an important test of the formalism.

We could have used the bare mass of any quark, in place of m_{0c}, in Eq. (3). Then the $n \geq 6$ moments would give values for the $\overline{\text{MS}}$ mass of that quark. Alternatively, we could leave the quark mass factor out, in which case these moments give the factors $Z_m(\mu)$ that convert any bare lattice quark mass into the corresponding $\overline{\text{MS}}$ mass at scale μ. Heavy-quark current-current correlators, as used here, provide an alternative to RI-mom [12] and similar methods for determining both light and heavy quark masses.

The new definition for the reduced moments simplifies our analysis since the variation of factor $m_c(\mu)$ with μ is

well known from perturbative QCD. The m_{η_h} dependence of the analogous factor $(m_{\eta_h}/2m_h)$ in the old analysis is unknown *a priori* and so must be modeled in the fit. We analyzed our data using the old definitions; the results, which agree with the results we find with the new methods, are described briefly in Appendix B.

B. Lattice simulations

To extract the coupling constant and c mass from simulations, we use the simulations to compute nonperturbative values for the reduced moments $\tilde{R}_n$ with small $n \geq 4$ and a range of heavy-quark masses m_{0h}. We vary the lattice spacing, so we can extrapolate to zero lattice spacing, and the sea-quark masses, so we can tune the masses to their physical values.

The gluon-field ensembles we use come from the MILC Collaboration and include u, d, s, and c quarks in the quark sea [13,14]. The parameters that characterize these ensembles are given in Table II. The highly accurate HISQ discretization [3] is used here for both the sea quarks and the heavy quarks in the currents used to create the correlators. This discretization was designed to minimize $(am_h)^2$ errors for large m_h. Our previous work used HISQ quarks in the currents, but a less accurate discretization (ASQTAD) for the sea quarks.

We also quote tuned values for the bare s and c quark masses in Table II. These are the quark masses that give the physical values for the η_s and η_c masses, as discussed in Appendix A 1. This is the bare c mass we use in Eq. (3) for $\tilde{R}_n$.

In Table III we list our simulation results for the η_h mass and the reduced moments for various bare quark masses am_{0h} on various ensembles. Results from different values of am_{0h} on the same ensemble are correlated; we include

TABLE II. Simulation parameters for the gluon ensembles used in this paper [13,14], with lattice spacings of approximately 0.15, 0.12, 0.09, and 0.06 fm, and various combinations of sea-quark masses. The parameters for each simulation are the inverse lattice spacing in units of $w_0 = 0.1715(9)$ fm, the spatial L and temporal T lattice lengths, the number of gluon configurations N_{cf} (each with multiple time sources), the bare sea-quark masses in lattice units $(am_{0\ell}, am_{0s}, am_{0c})$, and the tuned bare s and c quark masses in GeV. The tuned s and c masses give physical values for the η_s and η_c mesons, respectively. The ℓ mass is the average of the u and d masses, which are set equal in our simulations. $Z_m(\mu)$ is the ratio of the $\overline{\text{MS}}$ quark mass $m_q(\mu, n_f = 4)$ to the corresponding bare (lattice) mass m_{0q} (see Sec. II D). The last two entries for each ensemble indicate the degree to which the sea-quark masses are detuned (see Appendix A).

Ensemble	w_0/a	L/a	T/a	N_{cf}	$am_{0\ell}$	am_{0s}	am_{0c}	m_{0s}^{tuned}	m_{0c}^{tuned}	$Z_m(3\text{ GeV})$	$\delta m_{uds}^{\text{sea}}/m_s$	$\delta m_c^{\text{sea}}/m_c$
1	1.1119(10)	16	48	1020	0.01300	0.0650	0.838	0.0895(7)	1.138(4)	0.866(5)	0.228(16)	−0.058(8)
2	1.1272(7)	24	48	1000	0.00640	0.0640	0.828	0.0890(7)	1.130(4)	0.872(6)	0.046(14)	−0.050(8)
3	1.1367(5)	36	48	1000	0.00235	0.0647	0.831	0.0885(7)	1.125(4)	0.876(5)	−0.048(13)	−0.034(8)
4	1.3826(11)	24	64	300	0.01020	0.0509	0.635	0.0866(7)	1.057(3)	0.933(6)	0.236(16)	−0.044(8)
5	1.4029(9)	32	64	300	0.00507	0.0507	0.628	0.0861(7)	1.051(3)	0.938(6)	0.067(14)	−0.035(8)
6	1.4149(6)	48	64	200	0.00184	0.0507	0.628	0.0857(7)	1.047(3)	0.941(6)	−0.040(13)	−0.024(8)
7	1.9330(20)	48	96	300	0.00363	0.0363	0.430	0.0823(9)	0.977(3)	1.009(6)	0.104(11)	−0.021(8)
8	1.9518(7)	64	96	304	0.00120	0.0363	0.432	0.0818(7)	0.973(3)	1.013(6)	−0.011(13)	−0.003(8)
9	2.8960(60)	48	144	333	0.00480	0.0240	0.286	0.0778(7)	0.912(3)	1.080(7)	0.365(19)	0.045(9)

TABLE III. Simulation results for η_h masses and reduced moments with various bare heavy-quark masses am_{0h} and gluon ensembles (first column, see Table II). Only data for $am_{0h} \leq 0.8$ are used in fits to the correlators. The $\tilde{R}_n$ for $n \geq 6$ are in units of GeV^{-1}.

	am_{0h}	am_{η_h}	$\tilde{R}_4$	$\tilde{R}_6$	$\tilde{R}_8$	$\tilde{R}_{10}$
1	0.826	2.22510(10)	1.1627(1)	0.937(3)	0.885(3)	0.856(3)
	0.888	2.33188(9)	1.1477(1)	0.937(3)	0.893(3)	0.867(3)
2	0.818	2.21032(6)	1.1643(0)	0.943(3)	0.890(3)	0.860(3)
3	0.863	2.28770(4)	1.1528(0)	0.947(3)	0.900(3)	0.872(3)
4	0.645	1.83976(11)	1.1842(2)	0.986(3)	0.915(3)	0.874(2)
	0.663	1.87456(12)	1.1783(2)	0.988(3)	0.919(3)	0.880(2)
5	0.627	1.80318(8)	1.1896(1)	0.989(3)	0.915(3)	0.874(2)
	0.650	1.84797(8)	1.1819(1)	0.992(3)	0.921(3)	0.881(2)
	0.800	2.13055(7)	1.1409(1)	1.001(3)	0.951(3)	0.920(3)
6	0.637	1.82225(5)	1.1860(1)	0.994(3)	0.921(3)	0.880(2)
7	0.439	1.34246(4)	1.2134(1)	1.013(3)	0.921(3)	0.877(2)
	0.500	1.47051(4)	1.1886(1)	1.029(3)	0.946(3)	0.903(3)
	0.600	1.67455(4)	1.1565(1)	1.048(3)	0.978(3)	0.939(3)
	0.700	1.87210(4)	1.1315(0)	1.059(3)	1.002(3)	0.968(3)
	0.800	2.06328(3)	1.1118(0)	1.064(3)	1.019(3)	0.991(3)
8	0.433	1.32929(3)	1.2160(1)	1.015(3)	0.922(3)	0.877(2)
	0.500	1.47012(3)	1.1885(0)	1.033(3)	0.950(3)	0.906(2)
	0.600	1.67418(3)	1.1564(0)	1.052(3)	0.982(3)	0.943(3)
	0.700	1.87177(2)	1.1315(0)	1.063(3)	1.006(3)	0.972(3)
	0.800	2.06297(2)	1.1117(0)	1.068(3)	1.023(3)	0.995(3)
9	0.269	0.88525(5)	1.2401(4)	1.011(3)	0.913(3)	0.869(2)
	0.274	0.89669(5)	1.2368(4)	1.014(3)	0.917(3)	0.873(2)
	0.400	1.17560(5)	1.1752(2)	1.068(3)	0.985(3)	0.944(3)
	0.500	1.38750(4)	1.1440(2)	1.094(3)	1.023(3)	0.985(3)
	0.600	1.59311(4)	1.1204(1)	1.112(3)	1.051(3)	1.017(3)
	0.700	1.79313(4)	1.1018(1)	1.122(3)	1.073(3)	1.043(3)
	0.800	1.98751(3)	1.0867(1)	1.127(3)	1.088(3)	1.063(3)
	0.900	2.17582(3)	1.0823(0)	1.399(4)	1.246(3)	1.169(3)
	1.000	2.35773(3)	1.0284(0)	1.442(4)	1.295(4)	1.215(3)

these correlations in our analysis. The am_{η_h} values are computed from Bayesian fits of multistate function,

$$\sum_{j=1}^{10} b_j (e^{-m_j t} + e^{-m_j(T-t)}), \qquad (10)$$

to the correlators $G(t)$ for $t \geq 8$, where T is the temporal length of the lattice [15]. The fitting errors are small for am_{η_h} and have minimal impact on our final results.

The fractional errors in the $\tilde{R}_n$ for $n \geq 6$ are 20–40 times larger than those for $\tilde{R}_4$. This is because of the factor of $1/m_{0c}^{\text{tuned}}$ used in Eq. (3) to define these moments. As mentioned above, we could have used bare masses for other quarks in this definition to obtain values for their $\overline{\text{MS}}$ masses. Heavy-quark masses like m_{0c}, however, can usually be tuned more accurately than light-quark masses, as discussed in Appendix A. Masses for other quarks can be obtained from the c mass and nonperturbatively determined

quark mass ratios, as we show for the s and b masses in the next two sections.

As in our previous paper, we limit the maximum size of am_h in our analysis: we require $am_h \leq 0.8$. This keeps a^2 errors smaller than 10%.

We determine the lattice spacing by measuring the Wilson flow parameter w_0/a on the lattice (Table II) [16]. From previous simulations [17], we know that

$$w_0 = 0.1715(9) \text{ fm}, \qquad (11)$$

which we combine with our measured values of w_0/a to obtain the lattice spacing for each ensemble (Appendix A). This approach is far more accurate than that used in our earlier paper, which relied upon the r_1 parameter from the static-quark potential.

C. Fitting lattice data

Our goal is to find values for $\alpha_{\overline{\text{MS}}}(\mu)$ and $m_c(\mu)$ that make the theoretical results (from perturbation theory) for the reduced moments $\tilde{R}_n$ [Eqs. (5)–(6)] agree with the nonperturbative results from our simulations. We do this by simultaneously fitting results from all of our lattice spacings and quark masses for moments with $4 \leq n \leq 10$. To get good fits, we must correct the continuum formulas in Eqs. (5)–(6) for several systematic errors in the simulation. We fit the lattice data using the following corrected form:

$$\tilde{R}_n = \begin{cases} 1 & \text{for } n = 4 \\ 1/\xi_m m_c(\xi_\alpha \mu) & \text{for } n \geq 6 \end{cases} \qquad (12)$$

$$\times \, r_n(\alpha_{\overline{\text{MS}}}(\xi_\alpha \mu), \mu) \qquad (13)$$

$$\times \left(1 + d_n^{\text{cond}} \frac{\langle \alpha_s G^2/\pi \rangle}{(2m_h)^4} \right) \qquad (14)$$

$$\times \left(1 + d_n^{h,c} \frac{m_{0h}^2 - m_{0c}^2}{m_{0h}^2} \right) \qquad (15)$$

$$+ \left(\frac{am_{\eta_h}}{2.26} \right)^2 \sum_{i=0}^{N} c_i(m_{\eta_h}, n) \left(\frac{am_{\eta_h}}{2.26} \right)^{2i}. \qquad (16)$$

We use a Bayesian fit with priors for every fit parameter [15]. The priors are *a priori* estimates for the parameters based upon theoretical expectations and previous experience, especially from our earlier, very similar $n_f = 3$ analysis. In each case we test our choice of prior width against the Empirical Bayes Criterion [15], which in effect uses fluctuations in the data to suggest natural widths for priors. None of our priors is narrower than this optimal width, and most are wider, which leads to more conservative errors.

We now explain each part of the lattice formula in turn.

1. Detuned sea-quark masses

The terms $\alpha_{\overline{\text{MS}}}(\xi_\alpha \mu)$ and $\xi_m m_h(\xi_\alpha \mu)$ in $\tilde{R}_n$ are the $\overline{\text{MS}}$ coupling and heavy-quark mass for detuned sea-quark masses; see Eqs. (A9) and (A19) in Appendix A. Scale μ is chosen so that

$$\mu = 3\xi_m m_c(\xi_\alpha \mu) \frac{m_{0h}}{m_{0c}} = 3m_h(\mu, \delta m^{\text{sea}}). \quad (17)$$

Scale factors ξ_α and ξ_m are defined in Appendix A, which discusses how $\overline{\text{MS}}$ couplings and masses are affected by sea-quark masses. The coefficients g_α, $g_m \ldots$ in ξ_α and ξ_m are treated as fit parameters, with priors taken from the output of the fits described in the appendix.

The light sea-quark masses enter linearly in ξ_α and ξ_m, because of (nonperturbative) chiral symmetry breaking. Quark mass dependence also enters through the perturbation theory for the moments (r_n) but is quadratic in the mass and, therefore, negligible for light quarks.

2. μ dependence

The scale μ enters Eqs. (12)–(16) through the coupling constant $\alpha_{\overline{\text{MS}}}(\xi_\alpha \mu)$ and the c mass $m_c(\xi_\alpha \mu)$. We parametrize the coupling and mass in the fit by specifying their values at $\mu = 5$ GeV with fit parameters α_0 and m_0,

$$\alpha_{\overline{\text{MS}}}(5 \text{ GeV}, n_f = 4) = \alpha_0$$
$$m_c(5 \text{ GeV}, n_f = 4) = m_0, \quad (18)$$

whose priors are

$$\alpha_0 = 0.21 \pm 0.02, \qquad m_0 = 0.90 \pm 0.10. \quad (19)$$

Our previous analysis [2], converted from $n_f = 3$ to $n_f = 4$, gives 0.2134(24) and 0.8911(56) for these parameters; so the priors are broad. The coupling and mass for other values of μ are obtained by integrating (numerically) their evolution equations from perturbative QCD, starting from the values at $\mu = 5$ GeV:

$$\mu^2 \frac{d\alpha_{\overline{\text{MS}}}(\mu)}{d\mu^2} = -\beta_0 \alpha_{\overline{\text{MS}}}^2(\mu) - \beta_1 \alpha_{\overline{\text{MS}}}^3 - \beta_2 \alpha_{\overline{\text{MS}}}^4$$
$$- \beta_3 \alpha_{\overline{\text{MS}}}^5 - \beta_4 \alpha_{\overline{\text{MS}}}^6, \quad (20)$$

$$\frac{d\log m_h(\mu)}{d\log \mu^2} = -\gamma_0 \alpha_{\overline{\text{MS}}}(\mu) - \gamma_1 \alpha_{\overline{\text{MS}}}^2 - \gamma_2 \alpha_{\overline{\text{MS}}}^3$$
$$- \gamma_3 \alpha_{\overline{\text{MS}}}^4 - \gamma_4 \alpha_{\overline{\text{MS}}}^5. \quad (21)$$

The first four coefficients on the right-hand sides of these equations are known from perturbation theory [18–21]. In each case, we treat the fifth coefficient as a fit parameter whose prior's width equals the root-mean-square average of the first four parameters:

$$\beta_4 = 0 \pm \sigma_\beta, \qquad \gamma_4 = 0 \pm \sigma_\gamma. \quad (22)$$

Neither β_4 nor γ_4 has signficant impact on our final results.

3. Truncated perturbation theory

The Wilson coefficient function r_n [Eq. (13)] has a perturbative expansion of the form

$$r_n(\alpha_{\overline{\text{MS}}}, \mu) \equiv 1 + \sum_{j=1}^{N_{\text{pth}}} r_{nj}(\mu) \alpha_{\overline{\text{MS}}}^j. \quad (23)$$

The perturbative coefficients r_{nj} are known through third order and are given for $\mu = m_h(\mu)$ in Table I.

The lack of perturbative coefficients beyond third order is our largest single source of systematic error. Our data are sufficiently precise that higher-order terms are relevant. Furthermore, the relative importance of the higher-order terms varies with quark mass, as $\alpha_{\overline{\text{MS}}}$ varies with $\mu = 3m_h$. Therefore, we include the higher-order terms in our analysis with coefficients that we fit to account for variations with quark mass. As in our earlier analysis, we note that the known perturbative coefficients are small and relatively uncorrelated from moment to moment and order to order for $\mu = m_h$, leading us to adopt fit priors,

$$r_{nj}(\mu = m_h) = 0 \pm 1, \quad (24)$$

for the $n > 3$ coefficients at $\mu = m_h$. We double the width of these priors relative to our previous analysis because the fit suggested that some higher-order coefficients are larger here (especially for $n = 4$).

We set $N_{\text{pth}} = 15$ terms in the expansion, although our results are essentially unchanged once eight or more terms are included (or five with $\mu = m_h$). As before, we use renormalization group equations to express the coefficients $r_{nj}(\mu = 3m_h)$ in terms of the coefficients $r_{nj}(\mu = m_h)$ from Table I and Eq. (24). This procedure generates (correlated) priors for the unknown coefficients at $\mu = 3m_h$ that account for renormalization-group logarithms. The procedure makes our results largely independent of μ: our results change by less than a third of a standard deviation as μ is varied over the interval $2m_h \leq \mu \leq 10m_h$.

4. Nonperturbative effects: Finite-volume corrections

We use the Operator Product Expansion (OPE) in Eqs. (5)–(6) to separate short-distance from long-distance physics. In principle, the perturbative coefficients in $r_n(\alpha_{\overline{\text{MS}}}, \mu)$ above should have subtractions coming from the higher-order terms in the OPE expansion:

$$r_n \rightarrow r_n \left(1 - d_n^{\text{cond}} \frac{\langle \alpha_s G^2 / \pi \rangle_{\text{pth}}^{(\lambda)}}{(2m_h)^4} - \cdots \right), \quad (25)$$

where λ is a fixed cutoff scale in the perturbative regime, say $\lambda = 1$ GeV, and $\langle \alpha_s G^2/\pi \rangle_{\text{pth}}^{(\lambda)}$ and d_n^{cond} are computed in perturbation theory to the same order as r_n. These subtractions come from perturbative matching and remove contributions to r_n due to low-momentum gluons ($q \leq \lambda$), thereby also removing infrared renormalons order by order in perturbation theory. The size of the subtraction depends upon the detailed definition of $\alpha_s (G^{(\lambda)})^2$. This procedure is completely unambiguous given a specific definition for this operator, but we have not included the subtraction in r_n since it is negligible for any reasonable definition at our low orders of perturbation theory. For example, a simple momentum-space cutoff, that keeps $q^2 < \lambda^2$, gives [22]

$$\langle \alpha_s G^2 \rangle_{\text{pth}}^{(\lambda)} = \frac{3\alpha_s}{2\pi^3} \lambda^4, \tag{26}$$

which ranges from 0.001 to 0.019 GeV^4 for λs between 500 Mev and 1 GeV. This would change r_n by no more than 0.1%–0.4% at $m_h = m_c$ and much less at our higher m_hs.

Not surprisingly, perturbative estimates of the condensate value [Eq. (26)] are similar in size to nonperturbative estimates of the condensate value. So it is simpler for us to combine the subtraction in Eq. (25) with the condensate itself to form an effective condensate value [23]:

$$\langle \alpha_s G^2 \rangle_{\text{eff}} \equiv \langle \alpha_s G^2 \rangle^{(\lambda)} - \langle \alpha_s G^2 \rangle_{\text{pth}}^{(\lambda)}. \tag{27}$$

In our fits we take $\langle \alpha_s G^2 \rangle_{\text{eff}}$ as a fit parameter with prior

$$\langle \alpha_s G^2 \rangle_{\text{eff}} = 0.0 \pm 0.012, \tag{28}$$

and we approximate $m_h \approx m_{\eta_h}/2.26$ in the condensate correction (because $m_b(m_b) \approx m_{\eta_b}/2.26$). Our results are completely unchanged if the width of this prior is 10 times larger. In either case, we obtain a value for the effective condensate of order 0.002 with errors of a similar size. This is completely consistent with expectations, and it reduces condensate contributions to the moments to 0.01–0.05% at $m_h = m_c$, and much less at higher m_h—negligible at our level of precision.

This procedure is sensible at our level of precision. As precision increases, however, there is a point where it becomes important to remove renormalon corrections from the coefficients in r_n. Otherwise, $j!$ factors in jth order, coming from infrared renormalons, cause perturbation theory to diverge. A simple analysis [24] indicates that perturbation theory starts to diverge at order $j \sim 2/(\beta_0 \alpha_{\overline{\text{MS}}})$, which is around the eighth order for our analysis. Consequently we expect the impact of infrared renormalons to be negligible at third order.

Perturbation theory is not the whole story even if infrared renormalons are removed. The OPE separates short distances from long distances, but the short-distance coefficients r_n, d_n^{cond}... have nonperturbative contributions, for example, from small instantons [22]. It is also possible that the OPE is an asymptotic expansion and does not converge ultimately, although recent results suggest it might converge [25,26]. Whatever the case, such effects are expected to appear at even higher orders than infrared renormalons, and so are completely negligible at our level of precision.

Condensates, renormalons, small instantons, *etc.*, afflict all perturbative analyses at some level of precision. Our analysis is particularly insensitive to such effects because the leading nonperturbative contributions are suppressed by four powers of $\Lambda_{\text{QCD}}/(2m_h)$.

Note finally that the coefficient functions, being short-distance, are insensitive to errors caused by the finite volume of the lattice. While the finite volume *can* affect the value of $\langle \alpha_s G^2 \rangle_{\text{eff}}$, the impact on our results is negligible since the condensate itself is negligible. We verified this by recalculating the reduced moments for emsemble 5 in Table II with spatial lattice sizes of $L/a = 24$ and 40 (ensemble 5 uses 32). The moments for different volumes agree to within statistical errors of order 0.01%. The same is true for the measured values of m_{η_c} from these ensembles; finite volume effects will be smaller still for m_{η_h}.

5. $m_{0h} - m_{0c}$ correction

Our results are also affected by the difference between the c mass m_{0c} used in the sea and the mass of the heavy quark m_{0h} used to make the currents in the current-current correlator. The perturbative calculations we use assume $m_{0c} = m_{0h}$, but we want to study a range of m_{0h} values with fixed m_{0c}. The correction enters in $\mathcal{O}(\alpha_s^2)$, is quadratic in the mass difference for small differences, and goes to a (small) constant as $m_{0h} \to \infty$. Therefore, we correct for it using [Eq. (15)]

$$\tilde{R}_n \to \tilde{R}_n \left(1 + d_n^{h,c} \frac{m_{0h}^2 - m_{0c}^2}{m_{0h}^2} \right), \tag{29}$$

where h_n is a fit parameter with a prior of 0 ± 0.03. The width 0.03 is 10 times larger than the correct value (from perturbation theory) in the $m_{0h} \to \infty$ limit. It is twice as wide as the width indicated by the Empirical Bayes Criterion [15]. We also tried fits where $d_n^{h,c}$ was replaced by a spline function of m_{η_h}. These give similar results but with larger errors (especially for $\alpha_{\overline{\text{MS}}}$).

6. *Finite lattice spacing errors*

The final modification in our formula for $\tilde{R}_n$ corrects for errors caused by the finite lattice spacings used in the simulations. We write

$$\tilde{R}_n \to \tilde{R}_n + \delta \tilde{R}_n, \tag{30}$$

where

$$\delta\tilde{R}_n \equiv \left(\frac{am_{\eta_h}}{2.26}\right)^2 \sum_{i=0}^{N} c_i^{(n)}(m_{\eta_h})\left(\frac{am_{\eta_h}}{2.26}\right)^{2i}, \qquad (31)$$

and again $m_{\eta_h}/2.26$ is a proxy for the quark mass. We parametrize the m_{η_h} dependence of the $c_i^{(n)}(m_{\eta_h})$ using cubic splines with knots at

$$m_{\text{knots}} \equiv \{2.9, 3.6, 4.6, 7.9\} \text{ GeV} \qquad (32)$$

that come from the analysis in Sec. IV. We set

$$c_i^{(n)}(m) = c_{0i}^{(n)} + \delta c_i^{(n)}(m) \qquad (33)$$

with the following fit parameters and priors:

$$
\begin{aligned}
c_{0i}^{(n)} &= 0 \pm 1/n \\
\delta c_i^{(n)}(m) &= 0 \pm 0.10/n \qquad m \in m_{\text{knots}} \\
\delta c_i^{(n)\prime}(m) &= 0 \pm 0.10/n \qquad m = 2.9 \text{ GeV}. \quad (34)
\end{aligned}
$$

These priors are again conservative since the Empirical Bayes Criterion [15] suggests priors that are half as wide. We take $N = 20$, but our results are insensitive to any $N \geq 10$.

D. $n_f = 4$ lattice results

We fit all of the reduced moments from our simulation data—with lattice spacings from 0.12 fm to 0.06 fm, and $n = 4, 6, 8,$ and 10 in Table III—simultaneously to formula (12)–(16) by adjusting fit parameters described in the previous sections. The fit is excellent with a χ^2 per degree of freedom of 0.51 for 92 pieces of data (p value is 1.0).

The fit has two key physics outputs. One is a new result for the running coupling constant:

$$\alpha_{\overline{\text{MS}}}(5 \text{ GeV}, n_f = 4) = 0.2128(25). \qquad (35)$$

To compare with our old determination and other determinations, we use perturbation theory to add b quarks to the sea [27], with $m_b(m_b) = 4.164(23)$ GeV [2], and evolve to the Z mass (91.19 GeV) to get

$$\alpha_{\overline{\text{MS}}}(M_Z, n_f = 5) = 0.11822(74). \qquad (36)$$

This agrees well with 0.1183(7) from our $n_f = 3$ analysis [2]. It also agrees well with the current world average 0.1185(6) from the Particle Data Group [28].

The second important physics output is the c quark's mass, whose value at $\mu = 5$ GeV is a fit parameter:

$$m_c(\mu, n_f = 4) = \begin{cases} 0.8905(56) \text{ GeV} & \mu = 5 \text{ GeV} \\ 0.9851(63) \text{ GeV} & \mu = 3 \text{ GeV} \\ 1.2715(95) \text{ GeV} & \mu = m_c(\mu), \end{cases} \qquad (37)$$

where we have used Eq. (21) to evolve our result to other scales for comparison with other determinations. These again agree well with our previous $n_f = 3$ analysis [2], which gave 0.986(6) GeV for the mass at 3 GeV. The errors for $m_c(3 \text{ GeV})$ and $\alpha_{\overline{\text{MS}}}(M_Z)$ are correlated, with correlation coefficient 0.19.

We use our result from m_c to calculate the mass renormalization factors,

$$Z_m(\mu) \equiv \frac{m_c(\mu)}{m_{0c}}, \qquad (38)$$

that relate $\overline{\text{MS}}$ masses to bare lattice masses for each configuration. These factors can be used to convert the bare mass for any quark to its $\overline{\text{MS}}$ equivalent. We tabulate these results, with $\mu = 3$ GeV, for our configurations in Table II. These Z_m values are much more accurate than can be obtained from order α_s lattice QCD perturbation theory [29], but they agree qualitatively and suggest that higher-order corrections from lattice perturbation theory are small.

Our results confirm that a perturbative treatment of c quarks in the sea, as in our previous paper, is correct, at least to our current level of precision.

Our result at $\mu = m_c$ has a larger error because $\alpha_{\overline{\text{MS}}}$ in the mass evolution equation [Eq. (21)] becomes fairly large at that scale ($\alpha_{\overline{\text{MS}}} \approx 0.4$) and quite sensitive to uncertainties in its value. We use the coupling from our fit for this evolution. Were we instead to use the Particle Data Group's (more accurate) $\alpha_{\overline{\text{MS}}}$, our value for $m_c(m_c)$ would be

$$m_c(m_c, n_f = 4) = 1.2733(76) \text{ GeV}. \qquad (39)$$

In any case, it is probably better to avoid such low scales, if possible.

Note that our c mass comes from moments whose heavy-quark mass varies from $m_h = m_c$ to $m_h = 3m_c$. Each (nonperturbative) $\tilde{R}_n$ with $n \geq 6$, for each heavy-quark mass m_h, gives an independent estimate of the c mass:

$$m_c(3m_h) = \frac{r_n(\alpha_{\overline{\text{MS}}}(3m_h), \mu = 3m_h)}{\tilde{R}_n}. \qquad (40)$$

The extent to which these estimates agree with each other is shown in Fig. 1, where the nonperturbative results (data points) are compared with our best-fit result for $m_c(5 \text{ GeV})$ evolved perturbatively to other scales using Eq. (21) (gray band). As expected, finite a^2 errors are larger for smaller values of n and larger values of m_h [2,30]. Taking account of these errors, agreement between different determinations of the mass is excellent.

The dominant sources of error for our results are listed in Table IV. The most important systematics are due to the truncation of perturbation theory and our extrapolation to $a^2 = 0$. As in our previous analysis, the a^2 extrapolations are not large, as is clear from Fig. 1 and also Fig. 2. Also the
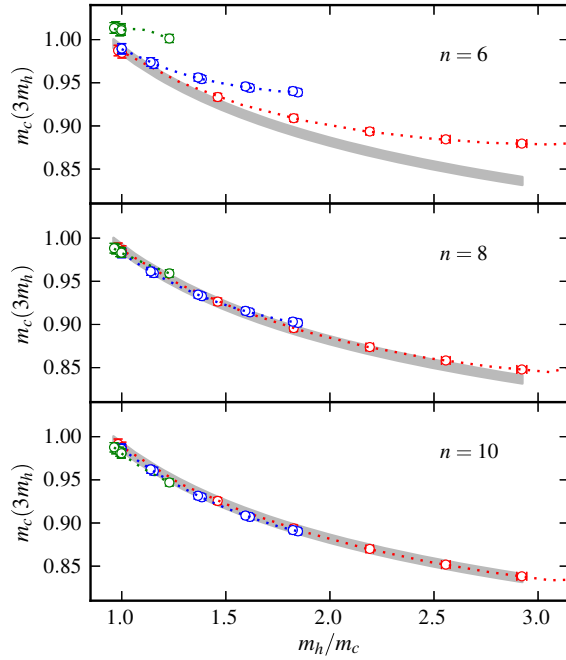
FIG. 1 (color online). The c quark mass $m_c(\mu = 3m_h)$ as determined from moments with heavy-quark masses ranging from m_c to $2.9m_c$. The data points show results obtained by substituting nonperturbative simulation values for $\tilde{R}_n$ into Eq. (40), after correcting for mistunings of the sea-quark masses (using the fit). Errors are about the size of the plot symbols, or smaller. Results are shown for three lattices spacings: 0.12 fm (green points, through $m_h/m_c = 1.2$), 0.09 fm (blue points, through $m_h/m_c = 1.8$), and 0.06 fm (red points, through $m_h/m_c = 2.9$). The dotted lines show our fits to these data points. The gray band shows the values expected from our best-value $m_c(5 \text{ GeV}) = 0.8905(56)$ GeV evolved perturbatively to the other scales.

TABLE IV. Error budget [31] for the c mass, QCD coupling, and the ratios of quark masses m_c/m_s and m_b/m_c from the $n_f = 4$ simulations described in this paper. Each uncertainty is given as a percentage of the final value. The different uncertainties are added in quadrature to give the total uncertainty. Only sources of uncertainty larger than 0.05% have been listed.

	$m_c(3)$	$\alpha_{\overline{\text{MS}}}(M_Z)$	m_c/m_s	m_b/m_c
Perturbation theory	0.3	0.5	0.0	0.0
Statistical errors	0.2	0.2	0.3	0.3
$a^2 \to 0$	0.3	0.3	0.0	1.0
$\delta m_{uds}^{\text{sea}} \to 0$	0.2	0.1	0.0	0.0
$\delta m_c^{\text{sea}} \to 0$	0.3	0.1	0.0	0.0
$m_h \neq m_c$ [Eq. (15)]	0.1	0.1	0.0	0.0
Uncertainty in w_0, w_0/a	0.2	0.0	0.1	0.4
α_0 prior	0.0	0.1	0.0	0.0
Uncertainty in m_{η_s}	0.0	0.0	0.4	0.0
$m_h/m_c \to m_b/m_c$	0.0	0.0	0.0	0.4
δm_{η_c}: electromag., annih.	0.1	0.0	0.1	0.1
δm_{η_b}: electromag., annih.	0.0	0.0	0.0	0.1
Total:	0.64%	0.63%	0.55%	1.20%

dependence of our results on the light sea-quark masses is quite small and independent of the lattice spacing, as illustrated by Fig. 3.

Our results change by $\sigma/3$ if we fit only the $n = 4$ and 6 moments, but the errors are 35% larger. Leaving out $n = 4$, instead, leaves the c mass almost unchanged, but increases the error in the coupling by 60% (with the same central value). We limit our analysis to heavy quark masses with $am_{0h} \leq 0.8$, as in our previous analysis. Reducing that limit to 0.7, for example, has no impact on the central values of results and increases our errors only slightly (less than 10%).

We tested the reliability of our error estimates for the perturbation theory by refitting our data using only a subset of the known perturbative coefficients. The results are presented in Fig. 4, which shows values for $m_c(3 \text{ GeV})$ and $\alpha_{\overline{\text{MS}}}(M_Z)$ from fits that treat perturbative coefficients beyond order N as fit parameters, with priors as in Eq. (24). Results from different orders agree with each other, providing evidence that our estimates of truncation

errors are reliable. This plot also shows the steady convergence of perturbation theory as additional orders are added.

As a further test of perturbation theory, we refit our nonperturbative data treating the leading perturbative coefficients, γ_0 and β_0, in the evolution equations for the mass [Eq. (21)] and coupling [Eq. (20)] as fit parameters with priors of 0 ± 1. The fit gives

$$\gamma_0 = 0.292(19) \qquad \beta_0 = 0.675(54), \qquad (41)$$

in good agreement with the exact results of 0.318 and 0.663, respectively. So our nonperturbative results for the correlators show clear evidence for the evolution of $m_c(\mu)$ and $\alpha_{\overline{\text{MS}}}(\mu)$ as $\mu = 3m_h$ varies from $3m_c$ to $9m_c$.
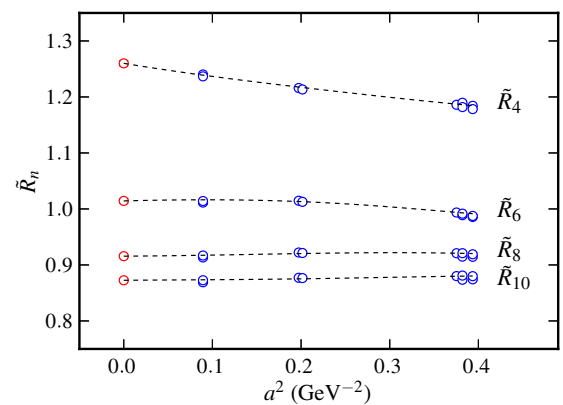

FIG. 2 (color online). Lattice-spacing dependence of reduced moments $\tilde{R}_n$ for η_h masses within 5% of m_{η_c}, and $n = 4, 6, 8, 10$. The dashed lines show our fit, and the points at $a = 0$ are the continuum extrapolations of the lattice data.
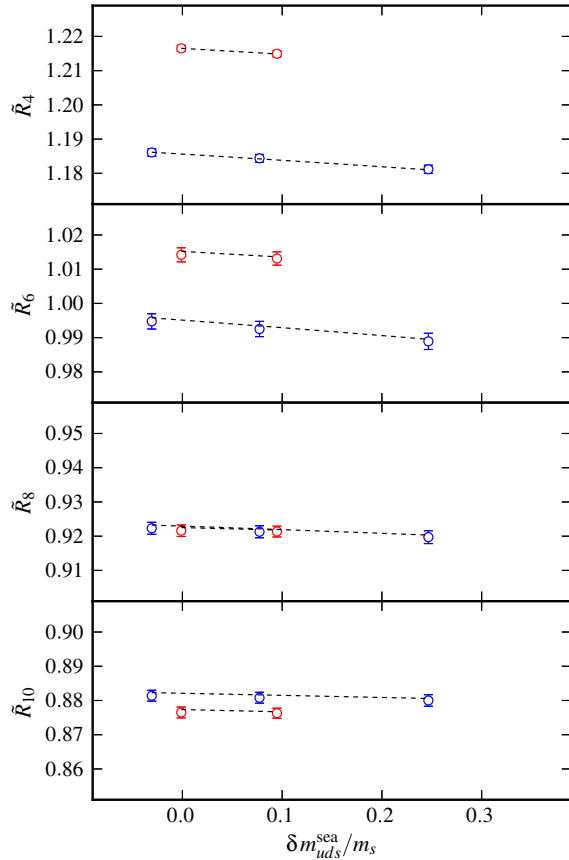
FIG. 3 (color online). Light sea-quark mass dependence of reduced moments $\tilde{R}_n$ for $m_h = m_c$, and $n = 4$, 6, 8, 10. Results are shown for our two coarsest lattices: $a = 0.12$ fm (three points in blue) and $a = 0.09$ fm (two points in red). The dashed lines show the corresponding results from our fit. Note that the slopes of the lines are independent of the lattice spacing, as expected.

III. m_c/m_s FROM $n_f = 4$

As discussed above (Sec. II A), we can use lattice QCD to extract ratios of $\overline{\text{MS}}$ quark masses completely non-perturbatively [32], since ratios of quark masses are scheme and scale independent, for example,

$$\frac{m_{0c}}{m_{0s}}\bigg|_{\text{lat}} = \frac{m_c(\mu, n_f)}{m_s(\mu, n_f)}\bigg|_{\overline{\text{MS}}} + \mathcal{O}((am_c)^2\alpha_s). \quad (42)$$

While ratios of light-quark masses can be obtained from chiral perturbation theory, only lattice QCD can produce nonperturbative ratios involving heavy quarks. These ratios are very useful for checking mass determinations that rely upon perturbation theory, as illustrated in [2]. They also allow us to leverage precise values of light-quark masses from very accurately determined heavy-quark masses.

In [32] we used nonperturbative simulations, with $n_f = 3$ sea quarks, to determine the s quark's mass from the c quark's mass and the ratio m_c/m_s. We repeat that analysis here, but now for $n_f = 4$ sea quarks, using the tuned values
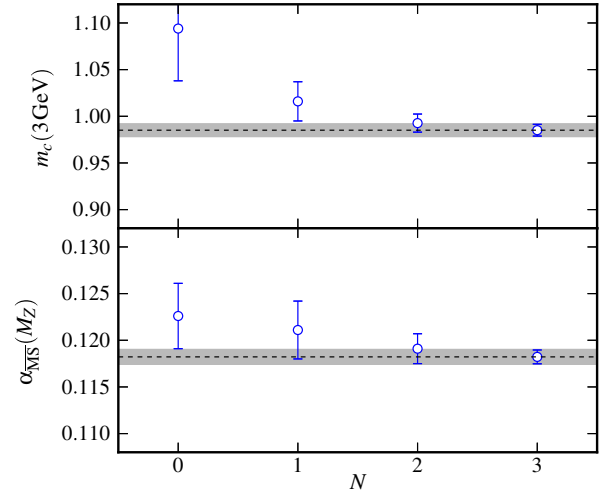

FIG. 4 (color online). Results for the $\overline{\text{MS}}$ c mass and coupling from $n_f = 4$ fits that treat perturbative coefficients beyond order N as fit parameters, with priors specified by Eq. (24). The gray bands and dashed lines indicate the means and standard deviations of our final results, which correspond to $N = 3$.

of the bare s and c masses for each of our lattice ensembles: am_{0s}^{tuned} and am_{0c}^{tuned} in Table II, respectively. We expect

$$\frac{am_{0c}^{\text{tuned}}}{am_{0s}^{\text{tuned}}} = \frac{m_c}{m_s}\left(1 + h_m\frac{\delta m_{uds}^{\text{sea}}}{m_s} + h_{a^2,m}\frac{\delta m_{uds}^{\text{sea}}}{m_s}\left(\frac{m_c}{\pi/a}\right)^2\right.$$
$$\left. + h_1\alpha_s(\pi/a)\left(\frac{m_c}{\pi/a}\right)^2 + \sum_{j=2}^{N_{a^2}}h_j\left(\frac{m_c}{\pi/a}\right)^{2j}\right), \quad (43)$$

where again we ignore δm_c^{sea} and δm^2 dependence since they are negligible. We fit the data from Table II using this formula with the following fit parameters and priors:

$$h_m = 0 \pm 0.1, \qquad h_{a^2,m} = 0 \pm 0.1, \quad (44)$$

$$h_1 = 0 \pm 6, \qquad h_j = 0 \pm 2 \quad (j > 1). \quad (45)$$

The extrapolated value m_c/m_s is also a fit parameter. We set $N_{a^2} = 5$, but get identical results for any $N_{a^2} \geq 2$.

The result of this fit is presented in Fig. 5, which shows the a^2 dependence of the lattice results. The sensitivity of our new results to a^2 is about half what we saw in our previous analysis. Our new fit is excellent and gives a final result for the mass ratio of

$$\frac{m_c(\mu, n_f)}{m_s(\mu, n_f)} = 11.652(65). \quad (46)$$

The leading sources of error in this result are listed in Table IV. These are dominated by statistical errors and uncertainty in the η_s mass. Many other potential sources of
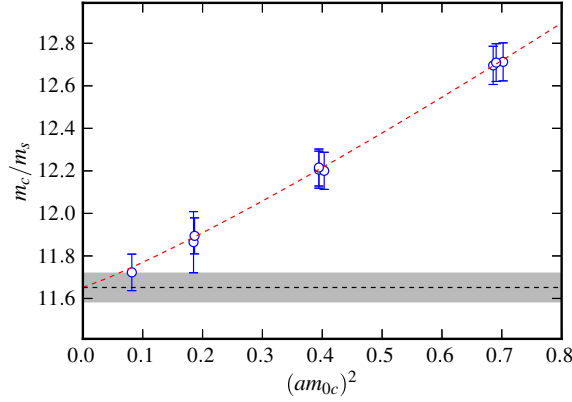
FIG. 5 (color online).   The ratio of the c and s quark masses as a function of the squared lattice spacing (in units of the bare c mass). The data come from simulations at lattice spacings of 0.15, 0.12, 0.09, and 0.06 fm, after tuning the s and c masses to reproduce physical values for the η_s and η_c masses on each ensemble. The errors for the data points are highly correlated, as they come primarily from uncertainties in w_0, m_{η_s}, and m_{η_c}. The red dashed line shows our fit, which has a χ^2 per degree of freedom of 0.21 for 9 degrees of freedom (p value of 0.99). The black dashed line and gray band show the mean value and standard deviation for our result extrapolated to zero lattice spacing.

error, such as uncertainties in the lattice spacing, largely cancel in the ratio.

Note that the discussion in Appendix A and Eq. (A19), in particular, imply that the leading effect of mistuned sea-quark masses cancels in ratios of quark masses. This is substantiated by our fit which makes parameter h_m negligibly small [−0.0080(34)]. Setting $h_m = 0$ shifts our result for m_c/m_s by only $\sigma/7$.

Our result is a little more than a standard deviation lower than the recent result, $11.747(19)(^{+59}_{-43})$, computed by the Fermilab/MILC Collaboration (using many of the same configurations we use) [33]. Our analysis uses a different scheme for tuning the lattice spacing and quark masses, which leads to the lack of sea-quark mass dependence in m_c/m_s discussed just above. The absence of sea-mass dependence is apparent from Fig. 5, where the clusters of data points correspond to ensembles with the same bare lattice coupling but different sea-quark masses. This figure can be compared with Fig. 6 in [33], which shows much larger sea-mass dependence. Both approaches should agree when extrapolated to zero lattice spacing and the physical sea-quark masses.

IV. m_h/m_c FROM m_{η_h}

An analysis similar to that in the previous section allows us to relate heavy-quark masses m_h to the $h\bar{h}$ pseudoscalar mass m_{η_h} with data from Table III. This can be used, for example, to estimate the b mass by extrapolating to m_{η_b}.
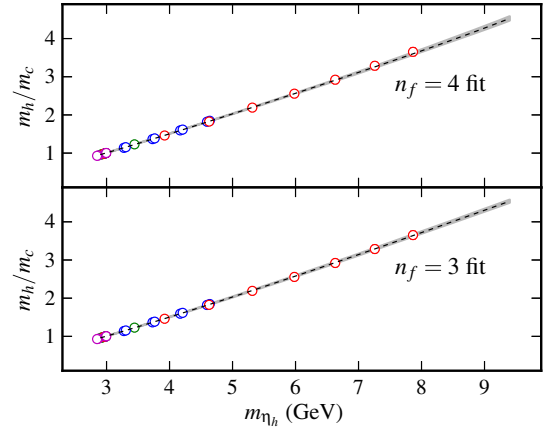

FIG. 6 (color online).   The ratio of the h and c quark masses as a function of the mass of $h\bar{h}$ pseudoscalar meson mass. The data come from simulations at lattice spacings of 0.15, 0.12, 0.09, and 0.06 fm; the data points are colored magenta, blue, green, and red, respectively. The gray band and dashed line in the top panel show function Eq. (47) with the best fit parameters, extrapolated to zero lattice spacing and the correct sea-quark masses. The bottom panel compares the $n_f = 4$ data with extrapolated results obtained in [2] from current-current correlators in $n_f = 3$ simulations.

Here we fit the lattice mass ratios $m_{0h}/m_{0c}^{\text{tuned}}$ to the following function of m_{η_h} from the simulation,

$$\frac{m_h}{m_c} = \frac{m_{\eta_h}}{m_{\eta_c}} \sum_{n=0}^{N} f_n(m_{\eta_h}) \left(\frac{am_{\eta_h}}{4}\right)^{2n} + f_{\text{sea}}(\eta_h) \frac{m_{\eta_h}}{m_{\eta_c}} \frac{\delta m_{uds}^{\text{sea}}}{m_s} \left(\frac{am_{\eta_h}}{4}\right)^2, \qquad (47)$$

where $N = 20$, although any $N > 3$ gives the same result. Here $f_n(m_{\eta_h})$ and $f_{\text{sea}}(m_{\eta_h})$ are cubic splines with knots at

$$m_{\text{knots}} = \{2.9, 3.6, 4.6, 7.9\} \text{ GeV}. \qquad (48)$$

The maximum and minimum knots correspond to the maximum and minimum values of m_{η_h}, while the locations of the internal knots were obtained by treating those locations as fit parameters. Each f is parametrized by

$$f(m) = f_0 + \delta f(m) \qquad (49)$$

and fit parameters

$$f_0 = 0 \pm 1$$
$$\delta f(m) = 0 \pm 0.15 \qquad m \in m_{\text{knots}}$$
$$\delta f'(m) = 0.15 \pm 0.15 \qquad m = 2.9 \text{ GeV}. \qquad (50)$$

We reduce the priors for the leading a^2 errors by a factor of $1/3$ since these errors are suppressed by α_s in the HISQ

discretization. The choice of priors for the spline parameters is motivated by results from [2] (see Fig. 4 in that paper).

The fit is excellent with a χ^2 per degree of freedom of 0.44 for 29 pieces of data: see the top panel in Fig. 6. Finite lattice spacing errors are much smaller for this quantity than for the moments, and it is again largely independent of mistunings in the sea-quark masses. Extrapolating to m_{η_b} gives

$$m_b/m_c = 4.528(54), \tag{51}$$

which agrees with our $n_f = 3$ result of 4.51(4), but with larger errors [2]. Our new $n_f = 4$ data go down to lattice spacings of 0.06 fm; our earlier analysis also had results at 0.045 fm.

The bottom panel of Fig. 6 compares our new $n_f = 4$ data with $n_f = 3$ results obtained from fits to the current-current correlators [2]. The agreement is excellent, showing again that $n_f = 3$ and $n_f = 4$ are consistent with each other.

V. CONCLUSIONS AND OUTLOOK

The initial extractions of quark masses from heavy-quark current-current correlators relied upon experimental data from $e\bar{e}$ annihilation [34,35]. Our analysis here, like the two that preceded it [2,30], replaces experimental data with nonperturbative results from tuned lattice simulations.

Lattice simulations offer several advantages over experiment for this kind of calculation [1]. For one thing, simulations are easier to instrument than experiments and much more flexible. Thus, we can generate lattice "data" not just for vector-current correlators but for any heavy-quark current or density; we optimize our simulations by using the pseudoscalar density instead of the vector current. Experiment provides results for only two heavy-quark masses—m_c and m_b—but we can produce lattice data for a whole range of masses between m_c and m_b. This means that $\alpha_{\overline{MS}}(\mu)$ varies continuously, by almost a factor of 2, in our analysis since $\mu \propto m_h$. Here we use this variation to estimate and bound uncalculated terms in perturbation theory, providing much more reliable estimates of perturbative errors than the standard procedure of replacing μ by $\mu/2$ and 2μ. (Our analysis is essentially independent of μ.) Nonperturbative contributions are also strongly dependent upon m_h and, therefore, more readily bound if a range of masses is available; they are negligible in our analysis.

In this paper, we have redone our earlier $n_f = 3$ analysis [2] using simulations with $n_f = 4$ sea quarks: u, d, s, and c. Our new results,

$$m_c(3 \text{ GeV}, n_f = 4) = 0.9851(63) \text{ GeV} \tag{52}$$

$$\alpha_{\overline{MS}}(M_Z, n_f = 5) = 0.11822(74), \tag{53}$$

agree well with our earlier results of 0.986(6) GeV and 0.1183(7), suggesting that contributions from c quarks in the sea are reliably estimated using perturbation theory (as expected). Our c mass is about 1.8σ lower than the recent result from the ETMC Collaboration, also using $n_f = 4$ simulations but with a different method [36]: they get $m_c(m_c) = 1.348(42)$ GeV, compared with our $n_f = 4$ result of 1.2715(95) GeV.

Our new result for the coupling [Eq. (53)] agrees with results from most other collaborations, who use different methods from us (and each other). Recent results ($n_f = 3$ or 4) are summarized in Fig. 7.

We updated our earlier $n_f = 3$ analysis [32] of the ratio m_c/m_s of quark masses using our $n_f = 4$ data. This is a relatively simple analysis of data from Table II. Our new value is

$$\frac{m_c(\mu, n_f)}{m_s(\mu, n_f)} = 11.652(65). \tag{54}$$

It agrees well with our previous result 11.85(16), but is much more accurate. We compare our new result with others in Fig. 8.

We obtain a new estimate for the s mass by combining our new result for m_c/m_s with our new estimate of the c mass (Eq. (52), converted from $n_f = 4$):

$$m_s(\mu, n_f = 3) = \begin{cases} 93.6(8) \text{ MeV} & \mu = 2 \text{ GeV} \\ 84.7(7) \text{ MeV} & \mu = 3 \text{ GeV}. \end{cases} \tag{55}$$

This brings the error below 1% for the first time. Values for $m_s(\mu, n_f = 4)$ are smaller by about 0.2 MeV. Our new result agrees with our previous analysis and also with other recent $n_f = 3$ or 4 analyses:
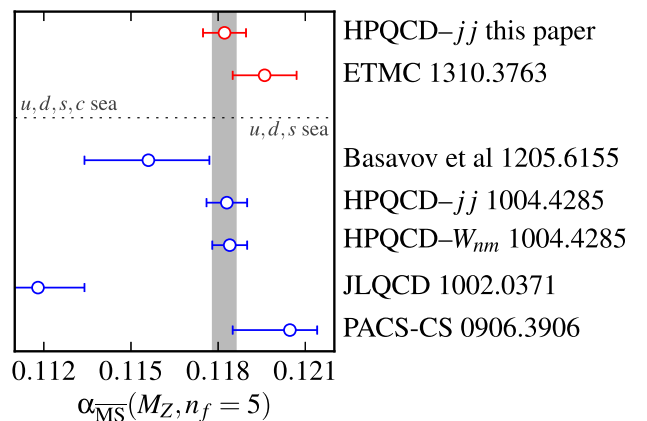

FIG. 7 (color online). Recent lattice QCD determinations of the QCD coupling ($n_f = 5$) evaluated at scale M_Z. The gray band is the weighted average of the results: 0.1182(4). We include our jj result for $n_f = 3$ in the average, but not our new $n_f = 4$ result since systematic errors are correlated between the two results. The results shown here come from this paper and [37–41].
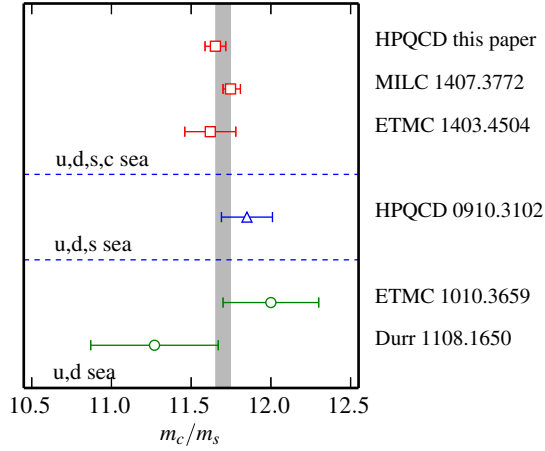
FIG. 8 (color online). Lattice QCD determinations of the ratio of the c and s quarks' masses. The ratios come from this paper and references [32,33,36,42,43]. The gray band is the weighted average of the three $n_f = 4$ results: 11.700(46).

$$m_s(2\text{ GeV}) = \begin{cases} 92.4(1.5)\text{ MeV} & \text{HPQCD}\,[32], \\ 99.6(4.3)\text{ MeV} & \text{ETMC}\,[36], \\ 95.5(1.9)\text{ MeV} & \text{Durr}\,et\,al.\,[44], \end{cases}$$

$$m_s(3\text{ GeV}) = 81.64(1.17)\text{ MeV} \quad \text{RBC/UKQCD}\,[45].$$

$$(56)$$

We compare these nonperturbative results in Fig. 9, together with an earlier perturbative determination from [44].

Finally, we have also updated our previous ($n_f = 3$) nonperturbative analysis of m_b/m_c using our new $n_f = 4$ data. We obtain

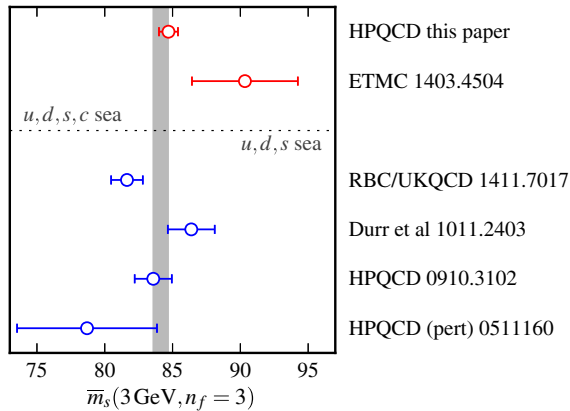$$\frac{m_b(\mu, n_f)}{m_c(\mu, n_f)} = 4.528(54), \qquad (57)$$

FIG. 9 (color online). Lattice QCD determinations of the $\overline{\text{MS}}$ s-quark mass $m_s(3\text{ GeV}, n_f = 3)$ in MeV. These masses come this paper and references [32,36,44–46] The gray band is the weighted average of these results: 84.1(5) MeV.

which agrees with our previous result of 4.51(4) [2]. Combining this result with our new value for m_c [Eq. (52)] gives

$$m_b(m_b, n_f = 5) = 4.162(48). \qquad (58)$$

This again agrees with our earlier result of 4.164(23) GeV, but with larger errors. We can also multiply our results for m_b/m_c and m_c/m_s to obtain

$$\frac{m_b(\mu, n_f)}{m_s(\mu, n_f)} = 52.55(55). \qquad (59)$$

This is almost four standard deviations (but only 4%) away from the result predicted by the Georgi-Jarlskog relationship [47] for certain classes of grand unified theory: the Georgi-Jarlskog relationship says that m_b/m_s should equal $3m_\tau/m_\mu = 50.45$.

The prospects for improving our results over the next decade are good. Detailed meta-simulations, described in [1], indicate that errors from our analysis can be pushed below 0.25% by a combination of higher-order perturbation theory, and, especially, smaller lattice spacings (0.045, 0.03, and 0.023 fm)—both improvements that are quite feasible over a decade [1]. There are also many other promising approaches within lattice QCD. Several exist already for extracting the QCD coupling; see, for example, [37–41,48,49]. One can also use simulations of other renormalized quantities, such as the $m_h \bar\psi_h \gamma_5 \psi$ vertex function, to compute quark masses [12].

Small lattice spacings are particularly important for the b mass, because lattice spacing errors are typically of order $(am_b)^2$. One approach is to use highly improved relativistic actions for the b quarks, like the HISQ action used here. As shown in [3], all but one of the $\mathcal{O}(a, a^2)$ operators that arise in the Symanzik improvement of a quark action are suppressed by extra factors of the heavy-quark velocity: factors of $(v/c)^2$ for mesons made of heavy quarks and v/c for mesons made of a combination of heavy and light quarks. The one operator that does not have extra suppression is $\sum_\mu \bar\psi \gamma^\mu (D^\mu)^3 \psi$, which violates Lorentz invariance and so is easily tuned nonperturbatively using the meson dispersion relation. This is the strategy adopted in the HISQ discretization we use here. The extra factors of v/c suppress $(am_b)^2$ errors by an extra order of magnitude, beyond the suppression, by a power of α_s, coming from tree-level corrections for a^2 errors in HISQ.

$(am_b)^2$ errors can be avoided completely by using effective field theories like NRQCD [50] or the Fermilab formalism [51] for b dynamics. Such approaches should be sufficiently accurate provided they are corrected to sufficiently high order in $(v_b/c)^2$. Our recent NRQCD analysis of m_b, using current-current correlators, is encouraging [52].

Overall, the prospects are excellent for continued improvement.

APPENDIX A: SEA-QUARK MASS DEPENDENCE

In this appendix we discuss the dependence of the $\overline{\rm MS}$ coupling and heavy-quark masses on the sea-quark masses. We vary the u/d sea-quark mass in our simulations to help us assess systematic errors associated with tuning that mass. In addition, the precision with which the s and c sea-quark masses have been tuned varies by several percent over the various ensembles we use. These detunings shift the $\overline{\rm MS}$ coupling and masses. We need to understand how they are shifted in order to extract results for $\alpha_{\overline{\rm MS}}$ and m_h with physical sea-quark masses.

It is essential when discussing detuned sea-quark masses to be specific about what is held fixed as the quark masses are shifted from their physical values. An obvious choice is to fix both the lattice spacing a and the bare coupling $\alpha_{\rm lat}$ in the lattice lagrangian, while varying the quark masses. We find it more convenient, however, to explore a slightly different manifold in theory space by fixing $\alpha_{\rm lat}$ and the value of the Wilson-flow parameter w_0.

Lattice simulations are done for particular values of the bare coupling constant (and bare quark masses) but with all dimensional quantities expressed in units of the lattice spacing (*lattice units*). This removes explicit dependence on the lattice spacing from the simulation, so we can run the simulation without knowing the lattice spacing. To extract physics, however, we must determine the lattice spacing (from the simulation) and convert all simulation results from lattice units to physical units. In our simulations, we calculate the lattice spacing by measuring the value of a/w_0 in the simulation and multiplying it by the known value of w_0 for physical sea-quark masses (that is, 0.1715(9) fm). As a result, the lattice spacing becomes (weakly) dependent upon the sea-quark masses since w_0 is affected by sea quarks.

This procedure is convenient because the lattice spacing for a given ensemble is determined using information from only that ensemble, thereby decoupling the analyses of different ensembles to a considerable extent. As we discuss below, there is an added benefit when vacuum polarization from c (or heavier) quarks is included in the simulation, as we do here: heavy quarks automatically decouple from low-energy physics (like w_0 [53]). With our procedure, physical quantities that probe energy scales smaller than $2m_c$—that is, almost everything studied with lattice QCD today—are essentially independent of m_c, which means that they are completely unaffected by tuning errors in m_c. This would not be the case if we fixed the lattice spacing instead of w_0, since it is small variations in the lattice spacing that correct for mistuning in m_c.

It is also very convenient that we set the lattice spacing using a flavor-singlet quantity. Because w_0 is a flavor singlet, the leading sea-mass dependence induced in the lattice spacing is analytic (linear) in the quark mass and small; in particular, there are no chiral logarithms [54]. One consequence is that leading-order chiral perturbation theory for physical quantities ($f_\pi, f_{D_s} \ldots$) is unchanged from standard treatments except for shifts (that are easily accommodated) in the coefficients of certain analytic terms.

In this appendix we show how the $\overline{\rm MS}$ coupling and heavy-quark mass depend upon the sea-quark masses in our simulations. This dependence implies sea-quark mass dependence in the lattice spacing and the heavy quark's bare mass, which we then use to determine some of the parameters involved. Finally, we review heavy-quark decoupling and estimate the parameters for c-mass dependence using first-order perturbation theory.

1. Tuning bare quark masses

We define tuned values for the bare c and s masses on each ensemble by adjusting those masses to give physical values in simulations for the η_c and η_s masses. The tuned values are listed in Table II.

The current experimental value for the η_c mass is 2.9836(7) GeV [28]. In our analysis, we remove electromagnetic corrections from this value and adjust its error to account for $c\bar{c}$ annihilation, since neither effect is in our simulations [55,56]. We use

$$m_{\eta_c}^{\rm phys} = 2.9863(27) \text{ GeV}. \tag{A1}$$

We compute the tuned c mass $m_{0c}^{\rm tuned}$ by linear interpolation using η_h masses from the simulation (Table III) for heavy-quark masses m_{0h} in the vicinity of m_{0c}. In a few cases, we have results for only a single value of m_{0h}; then we compute the tuned c mass using estimates of dm_{η_c}/dm_{0c} from other ensembles with (almost) the same lattice spacing.

Note that the uncertainty in $m_{0c}^{\rm tuned}$ is usually *smaller* than that in $am_{0c}^{\rm tuned}$. This is a peculiar feature of heavy-quark masses in lattice simulations (see, for example, [57]). It follows from the formula for the linear interpolation that defines the tuned mass in terms of a nearby mass,

$$m_{0c}^{\rm tuned} = (am_{0c})a^{-1} + \frac{dm_{0c}}{dm_{\eta_c}}(m_{\eta_c}^{\rm phys} - (am_{\eta_c})a^{-1}), \tag{A2}$$

where am_{η_c} is the simulation result for the η_c mass (in lattice units) when the c quark has mass am_{0c}. Here dm_{0c}/dm_{η_c} is obtained from simulation results for a few nearby c masses. The uncertainty in a^{-1} is usually larger than the uncertainties in the other lattice quantities, but here a^{-1} is multiplied by

$$(am_{0c}) - (am_{\eta_c})\frac{dm_{0c}}{dm_{\eta_c}}, \tag{A3}$$

which would vanish if $m_{\eta_c} = 2m_{0c}$. This cancellation is only partial for real masses, but it doesn't occur at all if Eq. (A2) is multiplied on both sides by a to give a formula for am_{0c}^{tuned}. As a result, fractional errors are roughly $3\times$ smaller for m_{0c}^{tuned}.

The η_s is an $s\bar{s}$ pseudoscalar particle where the valence quarks are (artificially) not allowed to annihilate; its physical mass is determined in lattice simulations from the masses of the pion and kaon [17]:

$$m_{\eta_s}^{\text{phys}} = 0.6885(22) \text{ GeV}. \tag{A4}$$

This mass is defined for use in lattice simulations and needs no further corrections for electromagnetism. We tune the s mass by simulating with a nearby bare mass m_{0s} to obtain the corresponding η_s mass and then extracting the tuned mass using

$$m_{0s}^{\text{tuned}} = m_{0s}\left(\frac{m_{\eta_s}^{\text{phys}}}{m_{\eta_s}}\right)^2. \tag{A5}$$

TABLE V. Simulation results for the η_s mass am_{η_s} corresponding to different values of the bare s mass am_{0s} and different gluon ensembles. The ensembles are described in Table II, although we use many more configurations for our η_s analysis than are indicated there. Estimates for the tuned bare s mass [Eq. (A5)] are also given.

Ensemble	am_{0s}	am_{η_s}	am_{0s}^{tuned}
1	0.0705	0.54024(15)	0.0700(9)
	0.0688	0.53350(17)	0.0700(9)
	0.0641	0.51511(16)	0.0700(9)
2	0.0679	0.52798(9)	0.0686(8)
	0.0636	0.51080(9)	0.0687(8)
3	0.0678	0.52680(8)	0.0677(8)
4	0.0541	0.43138(12)	0.0545(7)
	0.0522	0.42358(11)	0.0545(7)
5	0.0533	0.42637(6)	0.0533(7)
	0.0507	0.41572(14)	0.0534(7)
	0.0505	0.41474(8)	0.0534(7)
6	0.0527	0.42310(3)	0.0527(6)
	0.0507	0.41478(4)	0.0527(6)
8	0.0360	0.30480(4)	0.0364(4)
9	0.0231	0.20549(8)	0.0234(3)

Our η_s data are presented in Table V, which shows that the tuned mass is quite insensitive to small variations in m_{0s}. We do not have η_s results for ensemble 7; there, the tuned s mass is based on an interpolation between results from ensemble 8 and another ensemble that has similar parameters but with $am_{0\ell} = 0.0074$.

Table II shows that m_{0c}^{tuned} is more accurate than m_{0s}^{tuned}. This is because the uncertainties in the value of the lattice spacing have a smaller impact on the c mass because the cancellation described above only happens for heavy quarks (where $m_{\eta_h} \approx 2m_{0h}$).

We set the u and d masses equal to their average,

$$m_\ell \equiv \frac{m_u + m_d}{2}, \tag{A6}$$

and set m_ℓ equal to the tuned s mass (above) divided by the physical value of the quark mass ratio [33]

$$\frac{m_s}{m_\ell} = 27.35(11). \tag{A7}$$

2. $\alpha_{\overline{\text{MS}}}(\mu, \delta m^{\text{sea}})$ and $a(\delta m^{\text{sea}})$

The beta function in the $\overline{\text{MS}}$ scheme is, by definition, independent of sea-quark masses. Thus the coupling's evolution is unchanged by detuned sea-quark masses,

$$\frac{d\alpha_{\overline{\text{MS}}}(\mu, \delta m^{\text{sea}})}{d\log \mu^2} = \beta(\alpha_{\overline{\text{MS}}}(\mu, \delta m^{\text{sea}})), \tag{A8}$$

but mass dependence enters through the low-energy starting point for that evolution implied by the scale-setting procedure used in the lattice simulation. Such mass dependence can enter only through an overall renormalization of the scale parameter μ,

$$\alpha_{\overline{\text{MS}}}(\mu, \delta m^{\text{sea}}) = \alpha_{\overline{\text{MS}}}(\xi_\alpha \mu), \tag{A9}$$

where

$$\alpha_{\overline{\text{MS}}}(\mu) \equiv \alpha_{\overline{\text{MS}}}(\mu, \delta m^{\text{sea}} = 0) \tag{A10}$$

is the $\overline{\text{MS}}$ coupling for physical sea-quark masses. The scale factor,

$$\xi_\alpha \equiv 1 + g_\alpha \frac{\delta m_{uds}^{\text{sea}}}{m_s} + g_{a^2,\alpha} \frac{\delta m_{uds}^{\text{sea}}}{m_s}\left(\frac{m_c}{\pi/a}\right)^2$$
$$+ g_{c,\alpha}\frac{\delta m_c^{\text{sea}}}{m_c} + \mathcal{O}(\delta m^2), \tag{A11}$$

depends upon the differences between the masses m_q used in the simulation and the tuned values of those masses m_q^{tuned} (Table II and Sec. A 1):

$$\delta m_{uds}^{\text{sea}} \equiv \sum_{q=u,d,s} (m_q - m_q^{\text{tuned}}) \qquad (A12)$$

$$\delta m_c^{\text{sea}} \equiv m_c - m_c^{\text{tuned}}. \qquad (A13)$$

Function $\alpha_{\overline{\text{MS}}}(\xi_\alpha \mu)$ satisfies the standard evolution equation [Eq. (A8)] because ξ_α is independent of μ.

We work to first order in δm^{sea} because higher-order terms are negligible in our simulations. As suggested above, the leading-order dependence is particularly simple because we use iso-singlet mesons (η_c and η_s) to set the c and s masses; in particular, there are no chiral logarithms of the u/d mass in leading order.

We expect coefficients g_α and $g_{a^2,\alpha}$ in ξ_α to be of order $1/10$ since corrections linear in light-quark masses must be due to chiral symmetry breaking and so should be of order $\delta m^{\text{sea}}/\Lambda$ where $\Lambda \approx 10 m_s$. As we discuss below, $g_{c,\alpha}$ can be estimated from perturbation theory and is again of order $1/10$. We treat these coefficients as fit parameters in our analysis, with the following priors:

$$g_\alpha = 0 \pm 0.1, \qquad g_{a^2,\alpha} = 0 \pm 0.1, \qquad g_{c,\alpha} = 0 \pm 0.1. \qquad (A14)$$

The rescaling factor ξ_α is closely related to the dependence of the lattice spacing on the sea-quark masses used in the simulation. The lattice spacing is primarily a function of the bare coupling α_{lat} used in the lattice action, but it also varies with the sea-quark masses, in our scheme, when the bare coupling is held constant. As discussed above, this is because of sea-mass dependence in the quantity used to define the lattice spacing, a/w_0 in our case. The relationship with ξ_α can be understood by examining the $\overline{\text{MS}}$ coupling at scale $\mu = \pi/a$. There it is related to the bare coupling by a perturbative expansion,

$$\alpha_{\overline{\text{MS}}}(\pi/a, \delta m^{\text{sea}}) = \alpha_{\overline{\text{MS}}}(\xi_\alpha \pi/a)$$
$$= \alpha_{\text{lat}} + \sum_{n=2}^{\infty} c_n^{\overline{\text{MS}}} \alpha_{\text{lat}}^n, \qquad (A15)$$

that is mass independent up to corrections of $\mathcal{O}((am_c)^2\alpha_s)$, which are negligible in our analysis. This formula implies that $\alpha_{\overline{\text{MS}}}(\xi_\alpha \pi/a)$ is constant if α_{lat} is and, therefore, that ξ_α/a must be constant as well. Consequently, the lattice spacing must vary with δm^{sea} like

$$a(\delta m^{\text{sea}}) \approx \xi_\alpha a_{\text{phys}} \qquad (A16)$$

if the bare coupling is held constant, where a_{phys} is the lattice spacing when the sea-quark masses are tuned to their physical values, that is, $a_{\text{phys}} \equiv a(\delta m^{\text{sea}} = 0)$.

We use this variation in the lattice spacing to read off the parameters in ξ_α. Our simulation results fall into four groups of gluon ensembles, with lattice spacings around

0.15 fm, 0.12 fm, 0.09 fm, and 0.06 fm. Each group corresponds to a single value of the bare lattice coupling α_{lat}, and several different values of light sea-quark mass. Within a single group, then, the values we obtain for a/w_0 from our simulations should vary as

$$(a/w_0)_{\text{sim}} = \xi_\alpha \times (a/w_0)_{\text{phys}}, \qquad (A17)$$

where the parameters g_α, $g_{a^2,\alpha}$, and $g_{c,\alpha}$ in ξ_α [Eq. (A11)] are the same for all four groups of data.

We fit our simulation results for a/w_0, simultaneously for all four groups, as functions of g_α, $g_{a^2,\alpha}$, and $g_{c,\alpha}$. We also treat the value of $(a/w_0)_{\text{phys}}$ for each group as a fit parameter. The resulting fit is shown in Fig. 10 where we plot

$$\frac{(a/w_0)_{\text{sim}}}{(a/w_0)_{\text{phys}}}$$

versus $\delta m_{uds}^{\text{sea}}/m_s$.

The fit is excellent and shows that $g_\alpha = 0.082(8)$. Our fit is not very sensitive to $g_{a^2,\alpha}$ and $g_{c,\alpha}$—their impact on ξ_α is too small—and gives results for these that are essentially the same as the prior values.

3. $m_h(\mu, \delta m^{\text{sea}})$ and $m_{0c}(\delta m^{\text{sea}})$

The evolution equations for the heavy quark's $\overline{\text{MS}}$ mass are unchanged by sea-mass detunings:
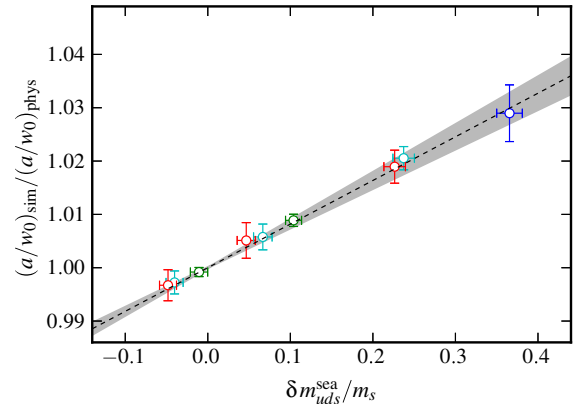

FIG. 10 (color online). The ratio of the simulation lattice spacing with detuned sea-quark masses to the lattice spacing with physical sea-quark masses as a function of the light-quark mass detuning (in units of the s quark mass). Results are shown for four different sets of data, each corresponding to a different bare lattice coupling. The approximate lattice spacings for these sets are: 0.15 fm (red points), 0.12 fm (cyan), 0.09 fm (green), and 0.06 fm (blue). The dashed line and gray band show the mean and standard deviation of our best fit to these data. The fit has a χ^2 per degree of freedom of 0.23 for 9 degrees of freedom (p value of 0.99).

$$\frac{d\log(m_h(\mu,\delta m^{\text{sea}}))}{d\log\mu^2} = \gamma_m(\alpha_{\overline{\text{MS}}}(\mu,\delta m^{\text{sea}})). \qquad (A18)$$

Consequently any sea-mass dependence must enter through rescalings,

$$m_h(\mu,\delta m^{\text{sea}}) = \xi_m m_h(\xi_\alpha \mu), \qquad (A19)$$

where ξ_α is defined above [Eq. (A11)], ξ_m is independent of μ, and

$$m_h(\mu) \equiv m_h(\mu, \delta m^{\text{sea}} = 0) \qquad (A20)$$

is the $\overline{\text{MS}}$ mass for physical sea-quark masses. We parametrize ξ_m similarly to ξ_α but allowing for the coefficients to depend upon the heavy-quark mass:

$$\xi_m = 1 + \frac{g_m}{(m_{\eta_h}/m_{\eta_c})^\zeta} \frac{\delta m^{\text{sea}}_{uds}}{m_s}$$
$$+ \frac{g_{a^2,m}}{(m_{\eta_h}/m_{\eta_c})^\zeta} \frac{\delta m^{\text{sea}}_{uds}}{m_s}\left(\frac{m_c}{\pi/a}\right)^2 + \cdots. \qquad (A21)$$

Again we expect g_m and $g_{a^2,m}$ to be of order $1/10$, and we treat them as fit parameters with the following priors:

$$g_m = 0 \pm 0.1, \qquad g_{a^2,m} = 0 \pm 0.1. \qquad (A22)$$

We parametrize the dependence on heavy-quark mass with the factors $(m_{\eta_h}/m_{\eta_c})^\zeta$ where ζ is a fit parameter with prior

$$\zeta = 0 \pm 1. \qquad (A23)$$

The sea-mass dependence in ξ_m comes from the quantity used to tune the heavy-quark mass in simulations. We tune these masses to give the correct physical mass for η_h—that is, the mass obtained when the sea-quark masses are tuned to their physical values and the lattice spacing is set to zero. This means that any sea-mass dependence in m_{η_h} is pushed into the rescaling factor ξ_m in Eq. (A19). The physical size of η_h mesons decreases as m_{η_h} increases, and this decreases the coupling with light sea-quarks. Thus we expect $\zeta > 0$ in Eq. (A21); our fit finds $\zeta = 0.3(1)$.

In principle, ξ_m should depend upon δm^{sea}_c, as well as $\delta m^{\text{sea}}_{uds}$. Perturbation theory, however, indicates that this dependence is negligible in our simulations. Thus we have omitted such terms from ξ_m. We have verified that they are negligible by comparing fits that include δm^{sea}_c terms with the fit without them.

The rescaling factor ξ_m is closely related to the sea-mass dependence of the heavy quark's bare mass, in much the same way as ξ_α is related to the lattice spacing. The bare mass m_{0h} is proportional to the $\overline{\text{MS}}$ mass evaluated at $\mu = \pi/a$:

$$m_{0h} \propto m_h(\pi/a, \delta m^{\text{sea}})$$
$$\propto \xi_m m_h(\xi_\alpha \pi/a). \qquad (A24)$$

Since ξ_α/a is sea-mass independent, we see that m_{h0} is proportional to ξ_m,

$$m_{0h}(\delta m^{\text{sea}}) = \xi_m m^{\text{phys}}_{0h}, \qquad (A25)$$

when the sea-quark masses are varied while holding the bare coupling fixed.

This variation can be used to determine the parameters in ξ_m, again in analogy to the previous section. As discussed in the previous section, our ensembles fall into four groups each corresponding to a different value of the bare coupling constant α_{lat}. The masses am^{tuned}_{0c} for each ensemble in Table II are tuned to give the physical η_c mass for that ensemble. Therefore, within each group of ensembles, we expect

$$am^{\text{tuned}}_{0c} = \xi_\alpha \xi_m \times (am_{0c})_{\text{phys}}, \qquad (A26)$$

where $(am_{0c})_{\text{phys}}$ is the value for properly tuned sea-quark masses.

We fit our simulation results for am^{tuned}_{0c} as functions of g_m, $g_{a^2,m}$, g_α, $g_{a^2,\alpha}$, and $g_{c,\alpha}$. We use best-fit values from the fit in the previous section as priors for the last three of these fit parameters. The values of $(am_{0c})_{\text{phys}}$ for the different groups of ensembles are also fit parameters.

The resulting fit is shown in Fig. 11, where we plot $am^{\text{tuned}}_{0c}/(am_{0c})_{\text{phys}}$ as a function of $\delta m^{\text{sea}}_{uds}/m_s$. The fit is
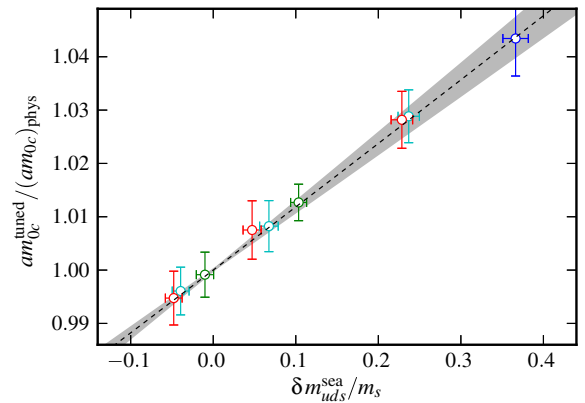

FIG. 11 (color online). The ratio of the bare c mass in lattice units used in the simulations to the bare mass with physical sea-quark masses as a function of the light-quark mass detuning (in units of the s quark mass). Results are shown for four different sets of data, each corresponding to a different bare lattice coupling. The approximate lattice spacings for these sets are: 0.15 fm (red points), 0.12 fm (cyan), 0.09 fm (green), and 0.06 fm (blue). The dashed line and gray band show the mean and standard deviation of our best fit to these data. The fit has a χ^2 per degree of freedom of 0.15 for 9 degrees of freedom (p value of 1.0).

excellent and shows that $g_m = 0.035(5)$, while $g_{a^2,m}$ is essentially unchanged from its prior value (because our data are not sufficiently accurate).

4. c quarks and decoupling

Heavy quarks decouple from low-energy physics, and therefore variations in δm_c^{sea} should have no impact on physics (like w_0) that probes momentum scales smaller than m_c. We can, however, introduce (apparent) violations of the decoupling theorem through the scheme used to set the lattice spacing. In particular, decoupling is violated by any scheme that holds the lattice spacing fixed (together with the bare coupling α_{lat}) as δm_c^{sea} is varied. On the contrary, decoupling is preserved by schemes that hold a low-energy ($< 2m_c$) quantity like w_0 fixed, instead of the lattice spacing [58].

The difference between these schemes arises because the running of the QCD coupling is modified in a detuned theory for scales between m_c^{sea} and $m_c^{\text{sea}} + \delta m_c^{\text{sea}}$, resulting in a mismatch between low and high energy values of the coupling. Physics below m_c is determined by the $n_f = 3$ coupling constant, which, by decoupling, should be independent of δm_c^{sea}.

To see how this works, we examine lowest-order perturbation theory where

$$\alpha_s^{(n_f)}(\mu) = \frac{2\pi}{\beta(n_f)\log(\mu/\Lambda^{(n_f)})} \tag{A27}$$

with $\beta(n_f) \equiv 11 - 2n_f/3$, and

$$\alpha_s^{(3)}(\mu) = \alpha_s^{(4)}(\mu, \delta m_c^{\text{sea}}) \tag{A28}$$

at $\mu = m_c + \delta m_c^{\text{sea}}$. Here $\Lambda^{(3)}$ must be independent of δm_c^{sea}, by decoupling, while $\Lambda^{(4)}$ must vary with δm_c^{sea} to cancel the effect of the shift in the match point $\mu = m_c + \delta m_c^{\text{sea}}$. It is straightforward to show that

$$\Lambda^{(4)}(\delta m_c^{\text{sea}}) \approx m_c \left(\frac{\Lambda^{(3)}}{m_c}\right)^{\beta(3)/\beta(4)} \left(1 - \frac{2}{25}\frac{\delta m_c^{\text{sea}}}{m_c}\right)$$

$$\approx \Lambda_{\text{phys}}^{(4)} \times \left(1 - \frac{2}{25}\frac{\delta m_c^{\text{sea}}}{m_c}\right), \tag{A29}$$

where $\Lambda_{\text{phys}}^{(4)}$ is the value for physical sea-quark masses. Thus, the decoupling theorem requires that

$$\alpha_s^{(4)}(\mu, \delta m_c^{\text{sea}}) = \alpha_s^{(4)}\left(\mu \times \left(1 + \frac{2}{25}\frac{\delta m_c^{\text{sea}}}{m_c}\right)\right). \tag{A30}$$

By comparing with Eqs. (A9) and (A11), we see that

$$g_{c,\alpha} = \frac{2}{25} + \mathcal{O}(\alpha_s), \tag{A31}$$

and, therefore, that the lattice spacing varies with δm_c^{sea} [Eq. (A16)].

There is an analogous effect in the heavy-quark mass, but the mass dependence in ξ_m is suppressed by α_s^2 and so is negligible in our analysis.

This analysis shows that a constant lattice spacing is incompatible with the decoupling theorem. The scheme we use avoids this problem by allowing the lattice spacing to vary with δm_c^{sea}, while holding the value of w_0 constant (as required by the decoupling theorem applied to w_0 itself). The violation of the decoupling theorem in the former case is only apparent; results from all schemes should agree when the sea-quark masses are tuned to their physical values.

APPENDIX B: PREVIOUS METHOD

The analysis in our previous ($n_f = 3$) paper used a different definition for the reduced moments with $n \geq 6$:

$$R_{n \geq 6} = \frac{m_{\eta_h}}{2m_{0h}}\left(G_n/G_n^{(0)}\right)^{1/(n-4)} \tag{B1}$$

instead of Eq. (3). As a result, these moments equal $z(m_{\eta_h}, \mu)r_n(\alpha_{\overline{\text{MS}}}, \mu)$ in perturbation theory, where

TABLE VI. Simulation results for η_h masses and reduced moments R_n (old definition) with various bare heavy-quark masses am_{0h} and gluon ensembles (first column, see Table II). Data from gluon ensembles 1–3 are not listed because they were not used in the analysis in Appendix B.

am_{0h}	am_{η_h}	R_4	R_6	R_8	R_{10}
4 0.645	1.83976(11)	1.1842(2)	1.4857(2)	1.3785(1)	1.3179(1)
0.663	1.87456(12)	1.1783(2)	1.4755(2)	1.3732(1)	1.3148(1)
5 0.627	1.80318(8)	1.1896(1)	1.4944(1)	1.3825(1)	1.3201(1)
0.650	1.84797(8)	1.1819(1)	1.4813(1)	1.3759(1)	1.3162(1)
0.800	2.13055(7)	1.1409(1)	1.4012(1)	1.3304(1)	1.2880(1)
6 0.637	1.82225(5)	1.1860(1)	1.4882(1)	1.3793(1)	1.3181(0)
7 0.439	1.34246(4)	1.2134(1)	1.5122(1)	1.3758(1)	1.3089(0)
0.500	1.47051(4)	1.1886(1)	1.4782(1)	1.3586(1)	1.2968(0)
0.600	1.67455(4)	1.1565(1)	1.4282(1)	1.3334(0)	1.2801(0)
0.700	1.87210(4)	1.1315(0)	1.3827(0)	1.3089(0)	1.2647(0)
0.800	2.06328(3)	1.1118(0)	1.3401(0)	1.2834(0)	1.2482(0)
8 0.433	1.32929(3)	1.2160(1)	1.5153(1)	1.3772(0)	1.3099(0)
0.500	1.47012(3)	1.1885(0)	1.4777(1)	1.3582(0)	1.2965(0)
0.600	1.67418(3)	1.1564(0)	1.4279(0)	1.3331(0)	1.2799(0)
0.700	1.87177(2)	1.1315(0)	1.3824(0)	1.3087(0)	1.2645(0)
0.800	2.06297(2)	1.1117(0)	1.3399(0)	1.2832(0)	1.2480(0)
9 0.269	0.88525(5)	1.2401(4)	1.5182(4)	1.3711(2)	1.3046(2)
0.274	0.89669(5)	1.2368(4)	1.5139(3)	1.3686(2)	1.3028(1)
0.400	1.17560(5)	1.1752(2)	1.4312(2)	1.3199(1)	1.2660(1)
0.500	1.38750(4)	1.1440(2)	1.3854(2)	1.2943(1)	1.2465(1)
0.600	1.59311(4)	1.1204(1)	1.3464(1)	1.2734(1)	1.2316(1)
0.700	1.79313(4)	1.1018(1)	1.3107(1)	1.2535(1)	1.2183(1)
0.800	1.98751(3)	1.0867(1)	1.2771(1)	1.2328(0)	1.2046(0)

$$z(m_{\eta_c}, \mu) \equiv \frac{m_{\eta_h}}{2m_h(\mu)} \qquad \text{(B2)}$$

replaces $z_c(\mu)$, which is defined at the c mass instead of m_h. Fits to these moments give both the coupling and the function $z(m_{\eta_h}, \mu)$, from which the c and b masses can be extracted.

We analyzed our data using the old definition, parametrizing the m_{η_h} dependence of $z(m_{\eta_c}, \mu)$ with a cubic spline. The values for the R_n moments used are given in Table VI. We obtained results that agree with the results obtained from our new method to within a standard deviation but are not quite as accurate:

$$\alpha_{\overline{\mathrm{MS}}}(5 \text{ GeV}, n_f = 4) = 0.2148(29) \qquad \text{(B3)}$$

$$m_c(3 \text{ GeV}, n_f = 4) = 0.9896(69). \qquad \text{(B4)}$$

The older method is more complicated because it attempts to determine the coupling at the same time as it determines the functional dependence of $z(m_{\eta_h}, \mu = 3m_h)$. In the new method, $z(m_{\eta_h}, \mu = 3m_h)$ is replaced by $z_c(\mu)$, whose dependence on μ is known *a priori* from perturbative QCD.

[1] For a review, see G. P. Lepage, P. B. Mackenzie, and M. E. Peskin, arXiv:1404.0319.

[2] C. McNeile, C. Davies, E. Follana, K. Hornbostel, and G. Lepage (HPQCD Collaboration), Phys. Rev. D **82**, 034512 (2010).

[3] E. Follana, Q. Mason, C. Davies, K. Hornbostel, G. Lepage, J. Shigemitsu, H. Trottier, and K. Wong (HPQCD Collaboration, UKQCD Collaboration), Phys. Rev. D **75**, 054502 (2007).

[4] A. Hart, G. von Hippel, and R. Horgan (HPQCD Collaboration), Phys. Rev. D **79**, 074008 (2009).

[5] M. A. Shifman, A. Vainshtein, and V. I. Zakharov, Nucl. Phys. **B147**, 385 (1979).

[6] K. Chetyrkin, J. H. Kuhn, and C. Sturm, Eur. Phys. J. C **48**, 107 (2006).

[7] R. Boughezal, M. Czakon, and T. Schutzmeier, Phys. Rev. D **74**, 074006 (2006).

[8] A. Maier, P. Maierhofer, and P. Marqaurd, Phys. Lett. B **669**, 88 (2008).

[9] Y. Kiyo, A. Maier, P. Maierhofer, and P. Marquard, Nucl. Phys. **B823**, 269 (2009).

[10] A. Maier, P. Maierhofer, P. Marquard, and A. Smirnov, Nucl. Phys. **B824**, 1 (2010).

[11] D. J. Broadhurst, P. A. Baikov, V. A. Ilyin, J. Fleischer, O. V. Tarasov, and V. A. Smirnov, Phys. Lett. B **329**, 103 (1994).

[12] G. Martinelli, C. Pittori, C. T. Sachrajda, M. Testa, and A. Vladikas, Nucl. Phys. **B445**, 81 (1995).

[13] A. Bazavov *et al.* (MILC Collaboration), Phys. Rev. D **82**, 074501 (2010).

[14] A. Bazavov *et al.* (MILC Collaboration), Phys. Rev. D **87**, 054505 (2013).

[15] G. Lepage, B. Clark, C. Davies, K. Hornbostel, P. B. Mackenzie, C. Morningstar, and H. Trottier, Nucl. Phys. B, Proc. Suppl. **106–107**, 12 (2002).

[16] S. Borsanyi, S. Durr, Z. Fodor, C. Hoelbling, S. D. Katz *et al.*, J. High Energy Phys. 09 (2012) 010.

[17] R. Dowdall, C. Davies, G. Lepage, and C. McNeile (HPQCD Collaboration), Phys. Rev. D **88**, 074504 (2013).

[18] T. van Ritbergen, J. Vermaseren, and S. Larin, Phys. Lett. B **400**, 379 (1997).

[19] M. Czakon, Nucl. Phys. **B710**, 485 (2005).

[20] J. Vermaseren, S. Larin, and T. van Ritbergen, Phys. Lett. B **405**, 327 (1997).

[21] K. Chetyrkin, Phys. Lett. B **404**, 161 (1997).

[22] V. Novikov, M. A. Shifman, A. Vainshtein, and V. I. Zakharov, Nucl. Phys. **B249**, 445 (1985).

[23] M. A. Shifman, Prog. Theor. Phys. Suppl. **131**, 1 (1998).

[24] See, for example, M. Shifman, arXiv:1310.1966.

[25] S. Hollands and C. Kopper, Commun. Math. Phys. **313**, 257 (2012).

[26] D. Pappadopulo, S. Rychkov, J. Espin, and R. Rattazzi, Phys. Rev. D **86**, 105043 (2012).

[27] K. Chetyrkin, B. A. Kniehl, and M. Steinhauser, Nucl. Phys. **B510**, 61 (1998).

[28] K. Olive *et al.* (Particle Data Group), Chin. Phys. C **38**, 090001 (2014) and 2013 partial update for the 2014 edition.

[29] C. McNeile, A. Bazavov, C. Davies, R. Dowdall, K. Hornbostel, G. Lepage, and H. Trottier, Phys. Rev. D **87**, 034503 (2013).

[30] I. Allison *et al.*, Phys. Rev. D **78**, 054513 (2008).

[31] The precise definition of our error budgets is described in Appendix A of C. Bouchard, G. P. Lepage, C. Monahan, H. Na, and J. Shigemitsu, Phys. Rev. D **90**, 054506 (2014).

[32] C. Davies, C. McNeile, K. Wong, E. Follana, R. Horgan, K. Hornbostel, G. P. Lepage, J. Shigemitsu, and H. Trottier (HPQCD Collaboration), Phys. Rev. Lett. **104**, 132003 (2010).

[33] A. Bazavov *et al.* (Fermilab Lattice and MILC Collaborations), arXiv:1407.3772.

[34] K. Chetyrkin, J. Kuhn, A. Maier, P. Maierhofer, P. Marquard, M. Steinhauser, and C. Sturm, Phys. Rev. D **80**, 074010 (2009);

[35] K. Chetyrkin, J. Kuhn, A. Maier, P. Maierhofer, P. Marquard, M. Steinhauser, and C. Sturm, Theor. Math. Phys. **170**, 217 (2012).

[36] N. Carrasco, A. Deuzeman, P. Dimopoulos, R. Frezzotti, V. Gimenez *et al.*, arXiv:1403.4504.

[37] B. Blossier, Ph. Boucaud, M. Brinet, F. De Soto, V. Morenas, O. Pène, K. Petrov, and J. Rodríguez-Quintero (ETM Collaboration), Phys. Rev. D **89**, 014507 (2014).

[38] A. Bazavov, N. Brambilla, X. Garcia i Tormo, P. Petreczky, J. Soto, and A. Vairo, Phys. Rev. D **86**, 114031 (2012).

[39] C. Davies, K. Hornbostel, I. Kendall, G. Lepage, C. McNeile, J. Shigemitsu, and H. Trottier (HPQCD Collaboration), Phys. Rev. D **78**, 114507 (2008).

[40] E. Shintani, S. Aoki, H. Fukaya, S. Hashimoto, T. Kaneko, T. Onogi, and N. Yamada, Phys. Rev. D **82**, 074505 (2010).Phys. Rev. D **89**, 099903 (2014).

[41] S. Aoki *et al.* (PACS-CS Collaboration), J. High Energy Phys. 10 (2009) 053.

[42] S. Durr and G. Koutsou, Phys. Rev. Lett. **108**, 122003 (2012).

[43] B. Blossier, P. Dimopoulos, R. Frezzotti, V. Lubicz, M. Petschlies, F. Sanfilippo, S. Simula, and C. Tarantino (ETM Collaboration), Phys. Rev. D **82**, 114513 (2010).

[44] Q. Mason, H. D. Trottier, R. Horgan, C. T. Davies, and G. P. Lepage (HPQCD Collaboration), Phys. Rev. **D73**, 114501 (2006).

[45] S. Durr, Z. Fodor, C. Hoelbling, S. Katz, S. Krieg *et al.*, Phys. Lett. **B701**, 265 (2011).

[46] T. Blum *et al.* (RBC Collaboration, UKQCD Collaboration), arXiv:1411.7017.

[47] H. Georgi and C. Jarlskog, Phys. Lett. **B86**, 297 (1979).

[48] K. Jansen, F. Karbstein, A. Nagy, and M. Wagner (ETM Collaboration), J. High Energy Phys. 01 (2012) 025.

[49] P. Fritzsch, F. Knechtli, B. Leder, M. Marinkovic, S. Schaefer, R. Sommer, and F. Virotta, Nucl. Phys. **B865**, 397 (2012).

[50] A. J. Lee, C. J. Monahan, R. R. Horgan, C. T. H. Davies, R. J. Dowdall, and J. Koponen (HPQCD Collaboration), Phys. Rev. D **87**, 074018 (2013).

[51] A. X. El-Khadra, A. S. Kronfeld, and P. B. Mackenzie, Phys. Rev. D **55**, 3933 (1997).

[52] B. Colquhoun, R. Dowdall, C. Davies, K. Hornbostel, and G. Lepage (HPQCD Collaboration), arXiv:1408.5768.

[53] Perturbation theory suggests that the important scales in w_0 are of order $Q_{w_0} = 1/\sqrt{8w_0^2} \approx 400$ MeV. See M. Luscher, J. High Energy Phys. 08 (2010) 071.

[54] O. Bär and M. Golterman, Phys. Rev. D **89**, 034505 (2014).

[55] C. Davies, C. McNeile, E. Follana, G. Lepage, H. Na, and J. Shigemitsu (HPQCD Collaboration), Phys. Rev. D **82**, 114504 (2010).

[56] E. B. Gregory, C. T. Davies, I. D. Kendall, J. Koponen, K. Wong *et al.* (HPQCD Collaboration), Phys. Rev. D **83**, 014506 (2011).

[57] C. Davies, K. Hornbostel, A. Langnau, G. Lepage, A. Lidsey, C. Morningstar, J. Shigemitsu, and J. Sloan, Phys. Rev. Lett. **73**, 2654 (1994).

[58] Dimensionless ratios of low-energy quantities are independent of the lattice-spacing scheme and must be independent of m_c by the decoupling theorem. This means that a scheme that makes any one low-energy quantity—for example, w_0—independent of m_c makes all other low-energy quantities independent of m_c, as well, thereby preserving decoupling.